

Size-Dependent Bending, Buckling and Free Vibration Analyses of Microscale Functionally Graded Mindlin Plates Based on the Strain Gradient Elasticity Theory

Abstract

In this paper, a size-dependent microscale plate model is developed to describe the bending, buckling and free vibration behaviors of microplates made of functionally graded materials (FGMs). The size effects are captured based on the modified strain gradient theory (MSGT), and the formulation of the paper is on the basis of Mindlin plate theory. The presented model accommodates the models based upon the classical theory (CT) and the modified couple stress theory (MCST) if all or two scale parameters are set to zero, respectively. By using Hamilton's principle, the governing equations and related boundary conditions are derived. The bending, buckling and free vibration problems are considered and are solved through the generalized differential quadrature (GDQ) method. A detailed parametric and comparative study is conducted to evaluate the effects of length scale parameter, material gradient index and aspect ratio predicted by the CT, MCST and MSGT on the deflection, critical buckling load and first natural frequency of the microplate. The numerical results indicate that the model developed herein is significantly size-dependent when the thickness of the microplate is on the order of the material scale parameters.

Keywords

Bending; Buckling; Free vibration; FGM microplate; Strain gradient theory; GDQ.

R. Ansari ^{* a}
 E. Hasrati ^a
 M. Faghieh Shojaei ^a
 R. Gholami ^b
 V. Mohammadi ^a
 A. Shahabodini ^a

^a Department of Mechanical Engineering
 University of Guilan, Rasht, Iran, P.O.
 Box 41635-3756

^b Department of Mechanical Engineering
 Lahijan Branch, Islamic Azad
 University, Lahijan, Iran, P.O. Box 1616

* Corresponding author; Tel. /fax: +98
 131 6690276. E-mail address:
r_ansari@guilan.ac.ir

<http://dx.doi.org/10.1590/1679-78252322>

Received 31.07.2015

In revised form 04.11.2015

Accepted 30.11.2015

Available online 05.01.2016

1 INTRODUCTION

The experiments conducted on the microstructures subjected to different loading conditions have revealed their size-dependent behavior (Nix 1989; Fleck et al. 1994; Ma and Clarke 1995; Vardoulakis et al. 1998; Stolken and Evans 1998; Chong and Lam 1999; Lam et al. 2003; and Colton 2005). When the dimensions of a structure are on the order of microns or submicrons, it

is necessary to consider internal material length scale parameters in order to predict its mechanical behavior. Conducting experiments on the microstructures is difficult and with high expenses. Hence, the continuum mechanics has attracted the attention of researchers for the modeling of microstructures. The classical continuum theories are not proper for identifying the behavior of small scale structures, because in such theories the character of stress is local with no material length scale. This shortcoming in the conventional continuum mechanics motivated some researchers to develop the non-classical theories taking the size effects into account.

One of the most significant higher-order continuum theories presented by Mindlin (1965) is gradient theory in which the first and second derivatives of the strain tensor effective on the strain energy density are included. Further, Fleck and Hutchinson (1993) extended Mindlin's theory and proposed the strain gradient theory which involves five material constants in the constitutive equations. In this theory, higher order stress components are appeared due to the stretch and rotation gradient tensors. Also, Toupin (1964), Mindlin and Tiersten (1962) used a higher order theory and developed the classical couple stress theory which included two material parameters. Determination of the material constants is one of the challenges these theories face. That's why; the works were done toward the modification of the mentioned theories and consequently, the reduction of the number of the length scale parameters involved. In this direction, the modified couple stress theory (MCST) was initiated by Yang et al (2002) in which only one length scale parameter is used in the constitutive equations leading to the symmetric couple stress tensor. Relevant works concerning the applicability of MCST in the analysis of microstructures can be found in (Ma et al. (2008); Tsiatas (2009); Kahrobaiyan et al. (2010); Ke et al. (2011); Jomehzadeh et al. (2011); Asghari (2012); Thai and Choi (2013)). In addition to these works, based on the modified couple stress and Kirchhoff plate theories, a size-dependent plate model was developed by Yin et al. (2010) for the dynamic analysis of microplate. Nateghi et al. (2012) employed the MCST and three different beam theories, i.e. classical, first and third order shear deformation beam theories to study the size effects on buckling load of functionally graded microbeams. Ke et al. (2012) studied the free vibrations of microplates on the basis of the modified couple stress and Mindlin plate theories.

Altan and Aifantis (1992) suggested a simplified strain gradient model including a single strain gradient coefficient of length squared dimension. Based on this model, Lazopoulos (2004) investigated the buckling behavior of a long rectangular plate subjected to uniaxial compression and small lateral load.

Lam et al. (2003) reduced five scale constants in strain gradient theory to three ones and presented the modified strain gradient theory. The constant are associated with dilatation gradient, deviatoric gradient and symmetric rotation gradient tensors so, this theory contains several higher-order stress components compared to the MCST.

Using the gradient elasticity theory, a higher-order Euler–Bernoulli beam model was developed by Papargyri-Beskou et al. (2003) and Kahrobaiyan et al. (2011). Papargyri-Beskou and Beskos (2008) presented a Kirchhoff microplate and conducted the static, stability and dynamic analysis of gradient elastic flexural plates. Lazopoulos (2009) employed the Kirchhoff plate theory and investigated the size effect on the bending of strain gradient elastic thin plates. Employing a variational method, Papargyri-Beskou et al. (2010) investigated the gradient elastic flexural Kirchhoff plate subjected to static loading and obtained the related boundary conditions. Wang et

al. (2011) did the static bending, instability and free vibration problems of an all edges simply supported rectangular micro-plate based on a size-dependent Kirchhoff micro-plate model. A comprehensive geometrically nonlinear size-dependent Timoshenko beam model was developed by Ansari et al. (2012) based on strain gradient and von Kármán theories. They applied the model and described the nonlinear free vibration of simply supported microbeam. Kahrobian et al. (2012) proposed a non-classical beam model accounting for the size influences in the framework of Euler–Bernoulli beam and strain gradient theories for static and free vibrations analyzes. They derived five equivalent length scale parameters in terms of the length scales of material constituents for functionally graded microbeams. Ansari et al. (2013) analyzed the pull-in instability of circular microplates based on the Kirchhoff plate theory and MSGT.

The novel thermo-mechanical properties of FGM make them as a prime candidate to be used in a wide range of engineering applications. These materials are also employed in the micro and nano-sized structures such as micro and nano–electromechanical systems and atomic force microscopes. Thus, to have a proper design of these systems, the knowledge of the mechanical behavior of FG microstructures is necessary. Recently, some research works have been conducted on the microscale structure made of functionally grade materials (Sahmani and Ansari (2013); Asghari et al. (2011); Ansari et al. (2011)).

In this paper, a non-classical size-dependent plate model is developed for the bending, buckling and free vibration analyses of microscale FG plates. The model takes the important size influences and the effect of transverse shear deformation into account through incorporating the strain gradient elasticity theory into the Mindlin plate theory. The constitutive relations of the present model have three length scale parameters, and for some specific values of the length scale material parameters, this model can be reduced to that based on the modified couple stress theory. Furthermore, the proposed model considers the influences of thermal environments on the static and dynamic responses of the FG microplates. Hamilton’s principle is utilized to derive the governing equations and corresponding boundary conditions. Also the current solution algorithm is based on the generalized differential quadrature (GDQ) method which enables one to impose any arbitrary boundary condition. So, in this work, the behavior of FG microscale plates with various edge conditions is studied. In the numerical results, the effects of different model parameters on the response of the microplate are investigated.

2 SIZE-DEPENDENT GOVERNING EQUATIONS AND BOUNDARY CONDITIONS

2.1 Modeling the Material Properties of FG Microplate

As shown in Fig. 1, an FG microplate having length a , width b and thickness h in a Cartesian coordinate system located at the midplane of the plate is considered. The bottom surface ($z = h/2$) of the plate is assumed to be rich-ceramic and the top surface ($z = -h/2$) is taken as rich-metal.

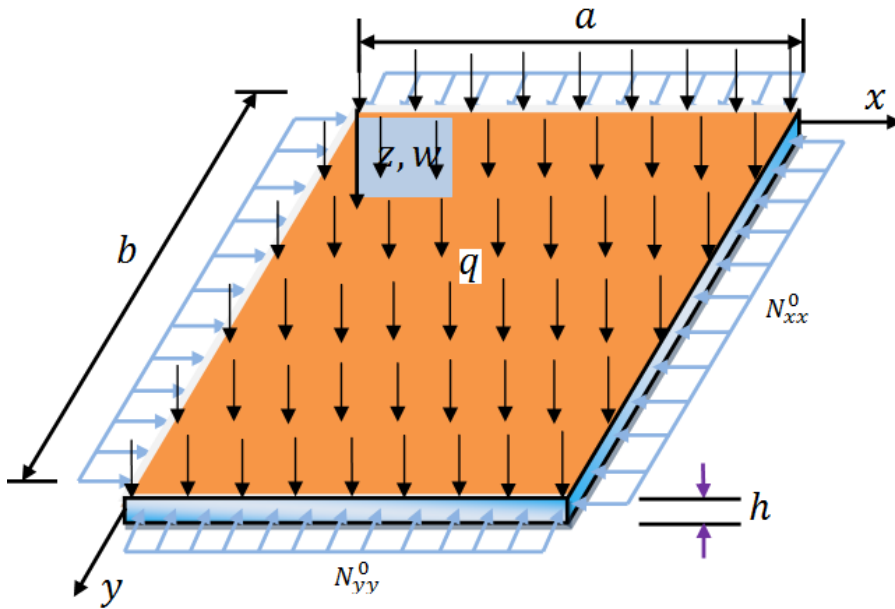


Figure 1: Schematic of an FG microplate under bi-axial loading and uniformly distributed transverse load: coordinate system and geometric parameters.

In the present work, the material properties of FGM, Young’s modulus E , Poisson’s ratio ν , mass density ρ , thermal conductivity K and thermal expansion coefficient α are taken to be of the following form

$$\begin{aligned}
 E(z) &= E_c V_c + E_m V_m, & \nu(z) &= \nu_c V_c + \nu_m V_m, & \rho(z) &= \rho_c V_c + \rho_m V_m \\
 \alpha(z) &= \alpha_c V_c + \alpha_m V_m, & K(z) &= K_c V_c + K_m V_m
 \end{aligned}
 \tag{1}$$

The volume fractions of ceramic and of metal, V_c and V_m respectively, are assumed to follow a power function of a spatial variable as

$$V_c(z) = \left(\frac{1}{2} + \frac{z}{h} \right)^{k_{FGM}}, \quad V_m = 1 - V_c
 \tag{2}$$

where k_{FGM} is the volume fraction or material gradient exponent. It is obvious that as the value of k_{FGM} approaches infinity the plate becomes fully metal and as it tends to zero the plate reduces to a fully ceramic one.

2.2 Kinematics of Microplate

Let $u(t, x, y)$, $v(t, x, y)$ and $w(t, x, y)$ denote the components of the displacement of a point located at the midplane of the plate along the x , y and z directions, respectively and ψ_x, ψ_y represent the angular displacements in the x and y directions, respectively. Based on the Mindlin plate theory, the

in-plane displacements are stated as linear functions of the plate thickness and the transverse deflection is considered to be constant along the plate thickness causing the displacement field to be expressed as

$$u_1 = u(t, x, y) - z\psi_x(t, x, y), \quad u_2 = v(t, x, y) - z\psi_y(t, x, y), \quad u_3 = w(t, x, y). \quad (3)$$

2.3 Constitutive Equations Based on the Modified Strain Gradient Theory

In comparison with the modified couple stress theory, the strain gradient theory proposed by Lam et al. (2003) includes two additional gradient tensors namely the dilatation gradient tensor and the deviatoric stretch gradient tensor. Assuming infinitesimal deformations, the strain energy Π_s stored in a continuum elastic medium occupying region Ω is expressed as

$$\Pi_s = \frac{1}{2} \int_{\Omega} (\sigma_{ij} \varepsilon_{ij} + p_i \gamma_i + \tau_{ijk}^{(1)} \eta_{ijk}^{(1)} + m_{ij}^s \chi_{ij}^s) d\Omega \quad (4)$$

where ε_{ij} , γ_i , $\eta_{ijk}^{(1)}$, χ_{ij}^s ($i, j, k = x, y, z$) denote the components of the strain tensor, the dilatation gradient tensor, the deviatoric stretch gradient tensor and the symmetric rotation gradient tensor, respectively given by

$$\varepsilon_{ij} = \frac{1}{2} (u_{i,j} + u_{j,i}) \quad (5-1)$$

$$\gamma_i = \varepsilon_{mm,i} \quad (5-2)$$

$$\eta_{ijk}^{(1)} = \eta_{ijk}^s - \frac{1}{3} (\delta_{ij} \eta_{mmk}^s + \delta_{jk} \eta_{mmi}^s + \delta_{ki} \eta_{mmj}^s); \quad \eta_{ijk}^s = \frac{1}{3} (\varepsilon_{jk,i} + \varepsilon_{ki,j} + \varepsilon_{ij,k}), \quad (5-3)$$

$$\chi_{ij}^s = \frac{1}{2} (\theta_{i,j} + \theta_{j,i}); \quad (5-4)$$

$$\theta_i = \frac{1}{2} (\text{curl}(u))_i \quad (5-5)$$

in which u_i, θ_i represent the components of the displacement vector \mathbf{u} and the infinitesimal rotation vector $\boldsymbol{\theta}$, respectively and the symbol δ denotes the Kronecker delta. The classical stress tensor σ_{ij} and the higher-order stresses $p_i, \tau_{ijk}^{(1)}, m_{ij}^s$ corresponding to a linear isotropic elastic material are stated as

$$\sigma_{ij} = \lambda \text{tr}(\boldsymbol{\varepsilon}) \delta_{ij} + 2\mu \varepsilon_{ij}, \quad p_i = 2\mu l_0^2 \gamma_i, \quad \tau_{ijk}^{(1)} = 2\mu l_1^2 \eta_{ijk}^{(1)}, \quad m_{ij}^s = 2\mu l_2^2 \chi_{ij}^s \quad (6)$$

l_0, l_1, l_2 represent the additional independent material length scale parameters associated with dilatation gradient, deviatoric stretch gradient and symmetric rotation gradient, respectively.

Furthermore, the parameters $\lambda = \frac{E\nu}{1-\nu^2}$ and $\mu = \frac{E}{2(1+\nu)}$ stand for the bulk and shear modules, respectively.

By substitution of Eqs. (3) into Eq. (5-5), one can get the components of infinitesimal rotation vector as

$$\theta_x = -\frac{1}{2}\left(\frac{\partial w}{\partial y} + \psi_y\right), \quad \theta_y = -\frac{1}{2}\left(\frac{\partial w}{\partial x} + \psi_x\right), \quad \theta_z = \frac{1}{2}\left(\frac{\partial v}{\partial x} - \frac{\partial u}{\partial y}\right) + \frac{z}{2}\left(\frac{\partial \psi_x}{\partial y} - \frac{\partial \psi_y}{\partial x}\right). \quad (7)$$

The nonzero components of the strain-displacement relations can be obtained by introducing Eq. (3) into Eq. (5-1), as

$$\begin{aligned} \epsilon_{xx} &= \frac{\partial u}{\partial x} - z \frac{\partial \psi_x}{\partial x}, & \epsilon_{yy} &= \frac{\partial v}{\partial y} - z \frac{\partial \psi_y}{\partial y}, & \epsilon_{xy} &= \frac{1}{2}\left(\frac{\partial u}{\partial y} + \frac{\partial v}{\partial x}\right) - \frac{z}{2}\left(\frac{\partial \psi_x}{\partial y} + \frac{\partial \psi_y}{\partial x}\right), \\ \epsilon_{xz} &= \frac{1}{2}\left(\frac{\partial w}{\partial x} - \psi_x\right), & \epsilon_{yz} &= \frac{1}{2}\left(\frac{\partial w}{\partial y} - \psi_y\right). \end{aligned} \quad (8)$$

The components of other three gradient tensors i.e., γ, η, χ are derived by introducing Eqs. (7) and (8) into Eqs. (5-2)-(5-4) as:

The dilatation gradient tensor:

$$\gamma_x = \frac{\partial^2 u}{\partial x^2} + \frac{\partial^2 v}{\partial x \partial y} - z\left(\frac{\partial^2 \psi_x}{\partial x^2} + \frac{\partial^2 \psi_y}{\partial x \partial y}\right), \quad \gamma_y = \frac{\partial^2 v}{\partial y^2} + \frac{\partial^2 u}{\partial x \partial y} - z\left(\frac{\partial^2 \psi_y}{\partial y^2} + \frac{\partial^2 \psi_x}{\partial x \partial y}\right), \quad \gamma_z = -\left(\frac{\partial \psi_x}{\partial x} + \frac{\partial \psi_y}{\partial y}\right). \quad (9)$$

The deviatoric stretch gradient tensor:

$$\begin{aligned} \eta_{xxx}^{(1)} &= \frac{1}{5}\left(2\frac{\partial^2 u}{\partial x^2} - \frac{\partial^2 u}{\partial y^2} - 2\frac{\partial^2 v}{\partial x \partial y}\right) - \frac{z}{5}\left(2\frac{\partial^2 \psi_x}{\partial x^2} - \frac{\partial^2 \psi_x}{\partial y^2} - 2\frac{\partial^2 \psi_y}{\partial x \partial y}\right), \\ \eta_{yyy}^{(1)} &= \frac{1}{5}\left(2\frac{\partial^2 v}{\partial y^2} - \frac{\partial^2 v}{\partial x^2} - 2\frac{\partial^2 u}{\partial x \partial y}\right) - \frac{z}{5}\left(2\frac{\partial^2 \psi_y}{\partial y^2} - \frac{\partial^2 \psi_y}{\partial x^2} - 2\frac{\partial^2 \psi_x}{\partial x \partial y}\right), \\ \eta_{zzz}^{(1)} &= \frac{2}{5}\left(\frac{\partial \psi_x}{\partial x} + \frac{\partial \psi_y}{\partial y}\right) - \frac{1}{5}\left(\frac{\partial^2 w}{\partial x^2} + \frac{\partial^2 w}{\partial y^2}\right), \\ \eta_{xxy}^{(1)} = \eta_{xyx}^{(1)} = \eta_{yxx}^{(1)} &= \frac{1}{15}\left(4\frac{\partial^2 v}{\partial x^2} + 8\frac{\partial^2 u}{\partial x \partial y} - 3\frac{\partial^2 v}{\partial y^2}\right) - \frac{z}{15}\left(8\frac{\partial^2 \psi_x}{\partial x \partial y} + 4\frac{\partial^2 \psi_y}{\partial x^2} - 3\frac{\partial^2 \psi_y}{\partial y^2}\right), \\ \eta_{xzz}^{(1)} = \eta_{zxx}^{(1)} = \eta_{zxx}^{(1)} &= \frac{1}{15}\left(4\frac{\partial^2 w}{\partial x^2} - \frac{\partial^2 w}{\partial y^2} - 8\frac{\partial \psi_x}{\partial x} + 2\frac{\partial \psi_y}{\partial y}\right), \\ \eta_{yyx}^{(1)} = \eta_{xyy}^{(1)} = \eta_{xyy}^{(1)} &= \frac{1}{15}\left(4\frac{\partial^2 u}{\partial y^2} - 3\frac{\partial^2 u}{\partial x^2} + 8\frac{\partial^2 v}{\partial x \partial y}\right) - \frac{z}{15}\left(8\frac{\partial^2 \psi_y}{\partial x \partial y} + 4\frac{\partial^2 \psi_y}{\partial y^2} - 3\frac{\partial^2 \psi_x}{\partial x^2}\right), \end{aligned} \quad (10)$$

$$\eta_{yyz}^{(1)} = \eta_{zyy}^{(1)} = \eta_{zyy}^{(1)} = \frac{1}{15} \left(4 \frac{\partial^2 w}{\partial y^2} - \frac{\partial^2 w}{\partial x^2} + 2 \frac{\partial \psi_x}{\partial x} - 8 \frac{\partial \psi_y}{\partial y} \right),$$

$$\eta_{zzx}^{(1)} = \eta_{zxx}^{(1)} = \eta_{xzz}^{(1)} = -\frac{1}{15} \left(3 \frac{\partial^2 u}{\partial x^2} + 2 \frac{\partial^2 v}{\partial x \partial y} + \frac{\partial^2 u}{\partial y^2} \right) + \frac{z}{15} \left(3 \frac{\partial^2 \psi_x}{\partial x^2} + 2 \frac{\partial^2 \psi_y}{\partial x \partial y} + \frac{\partial^2 \psi_x}{\partial y^2} \right),$$

$$\eta_{zzy}^{(1)} = \eta_{zyz}^{(1)} = \eta_{yzz}^{(1)} = -\frac{1}{15} \left(\frac{\partial^2 v}{\partial x^2} + 3 \frac{\partial^2 v}{\partial y^2} + 2 \frac{\partial^2 u}{\partial x \partial y} \right) + \frac{z}{15} \left(\frac{\partial^2 \psi_y}{\partial x^2} + 3 \frac{\partial^2 \psi_y}{\partial y^2} + 2 \frac{\partial^2 \psi_x}{\partial x \partial y} \right),$$

$$\eta_{xyz}^{(1)} = \eta_{yzx}^{(1)} = \eta_{zxy}^{(1)} = \eta_{xzy}^{(1)} = \eta_{yxz}^{(1)} = \eta_{zyx}^{(1)} = \frac{1}{3} \left(\frac{\partial^2 w}{\partial x \partial y} - \frac{\partial \psi_x}{\partial y} - \frac{\partial \psi_y}{\partial x} \right)$$

The symmetric rotation gradient tensor:

$$\chi_{xx}^s = \frac{1}{2} \left(\frac{\partial^2 w}{\partial x \partial y} + \frac{\partial \psi_y}{\partial x} \right), \chi_{yy}^s = -\frac{1}{2} \left(\frac{\partial^2 w}{\partial x \partial y} + \frac{\partial \psi_x}{\partial y} \right), \chi_{zz}^s = \frac{1}{2} \left(\frac{\partial \psi_x}{\partial y} - \frac{\partial \psi_y}{\partial x} \right),$$

$$\chi_{xy}^s = \frac{1}{4} \left(\frac{\partial^2 w}{\partial y^2} - \frac{\partial^2 w}{\partial x^2} + \frac{\partial \psi_y}{\partial y} - \frac{\partial \psi_x}{\partial x} \right), \chi_{xz}^s = \frac{1}{4} \left(\frac{\partial^2 v}{\partial x^2} - \frac{\partial^2 u}{\partial x \partial y} \right) + \frac{z}{4} \left(\frac{\partial^2 \psi_x}{\partial x \partial y} - \frac{\partial^2 \psi_y}{\partial x^2} \right),$$

$$\chi_{yz}^s = \frac{1}{4} \left(\frac{\partial^2 v}{\partial x \partial y} - \frac{\partial^2 u}{\partial y^2} \right) + \frac{z}{4} \left(\frac{\partial^2 \psi_x}{\partial y^2} - \frac{\partial^2 \psi_y}{\partial x \partial y} \right).$$
(11)

On substitution of Eqs. (8)-(11) into (6), the constitutive equations corresponding to the classical and strain gradient theories are obtained.

2.4 Derivation of General Form of Governing Equations and Boundary Conditions

The microplate is first considered to be subjected to the in-plane prebuckling forces N_{xx}^0 , N_{yy}^0 and N_{xy}^0 and the transverse load $q(t, x, y)$ as shown in Fig. 1. Herein, to derive the equations of motion, Hamilton's principle is employed which is expressed as follows

$$\delta \int_{t_1}^{t_2} (\Pi_T - \Pi_s + \Pi_w) dt = 0, \quad (12)$$

where Π_T and Π_w are the kinetic energy of FG microplate and the work done by the external loads, respectively. From Eq. (4), the total strain energy can be written as the addition of strain energies corresponding to the classical stresses Π_C , the dilatation stresses Π_{NC1} , the deviatoric stretch stresses Π_{NC2} and the couple stresses Π_{NC3} as

$$\Pi_s = \Pi_C + \Pi_{NC1} + \Pi_{NC2} + \Pi_{NC3} \quad (13)$$

The normal resultant forces, shear forces, bending moments and couple moments are related to the components of classical and the couple stress tensors as follows

$$\left(N_{xx}, N_{yy}, N_{xy}, Q_x, Q_y \right) = \int_{-h/2}^{h/2} (\sigma_{xx}, \sigma_{yy}, \sigma_{xy}, k_s \sigma_{xz}, k_s \sigma_{yz}) dz, \tag{14-1}$$

$$\left(M_{xx}, M_{yy}, M_{xy} \right) = \int_{-h/2}^{h/2} (\sigma_{xx}, \sigma_{yy}, \sigma_{xy}) z dz, \tag{14-2}$$

$$\left(Y_{xx}, Y_{yy}, Y_{zz}, Y_{xy}, Y_{xz}, Y_{yz} \right) = \int_{-h/2}^{h/2} \left(m_{xx}^s, m_{yy}^s, m_{zz}^s, m_{xy}^s, m_{xz}^s, m_{yz}^s \right) dz, \tag{14-3}$$

$$\left(H_{xz}, H_{yz} \right) = \int_{-h/2}^{h/2} \left(m_{xz}^s, m_{yz}^s \right) z dz, \tag{14-4}$$

where k_s denotes the shear correction factor.

The effective higher order stresses on a section defined above lead to the higher-order resultants force and moments in the section which are stated as

$$\left(P_x, P_y, P_z \right) = \int_{-h/2}^{h/2} \left(p_x, p_y, p_z \right) dz \tag{15-1}$$

$$\left(T_{xxx}, T_{yyy}, T_{zzz}, T_{xxy}, T_{xxz}, T_{yyx}, T_{yyz}, T_{xyz} \right) = \int_{-h/2}^{h/2} \left(\tau_{xxx}^{(1)}, \tau_{yyy}^{(1)}, \tau_{zzz}^{(1)}, \tau_{xxy}^{(1)}, \tau_{xxz}^{(1)}, \tau_{yyx}^{(1)}, \tau_{yyz}^{(1)}, \tau_{xyz}^{(1)} \right) dz \tag{15-2}$$

$$\left(M_x^p, M_y^p \right) = \int_{-h/2}^{h/2} \left(p_x, p_y \right) z dz, \left(M_{xxx}, M_{yyy}, M_{xxy}, M_{yyx} \right) = \int_{-h/2}^{h/2} \left(\tau_{xxx}^{(1)}, \tau_{yyy}^{(1)}, \tau_{xxy}^{(1)}, \tau_{yyx}^{(1)} \right) z dz \tag{15-3}$$

The strain energies associated with the classical elastic theory and strain gradient theory appeared in Eq. (13) can be obtained by using Eqs. (14) and (15) as

$$\begin{aligned} \Pi_C = \frac{1}{2} \int_{\Omega} \sigma_{ij} \varepsilon_{ij} d\Omega = \frac{1}{2} \int_A \left\{ N_{xx} \frac{\partial u}{\partial x} - M_{xx} \frac{\partial \psi_x}{\partial x} + N_{yy} \frac{\partial v}{\partial y} - M_{yy} \frac{\partial \psi_y}{\partial y} + N_{xy} \left(\frac{\partial u}{\partial y} + \frac{\partial v}{\partial x} \right) \right. \\ \left. - M_{xy} \left(\frac{\partial \psi_x}{\partial y} + \frac{\partial \psi_y}{\partial x} \right) + Q_x \left(\frac{\partial w}{\partial x} - \psi_x \right) + Q_y \left(\frac{\partial w}{\partial y} - \psi_y \right) \right\} dA, \end{aligned} \tag{16-1}$$

$$\begin{aligned} \Pi_{NC1} = \frac{1}{2} \int_{\Omega} p_i \gamma_i d\Omega = \frac{1}{2} \int_A \left\{ P_x \left(\frac{\partial^2 u}{\partial x^2} + \frac{\partial^2 v}{\partial x \partial y} \right) - M_x^p \left(\frac{\partial^2 \psi_x}{\partial x^2} + \frac{\partial^2 \psi_y}{\partial x \partial y} \right) + P_y \left(\frac{\partial^2 v}{\partial y^2} + \frac{\partial^2 u}{\partial x \partial y} \right) \right. \\ \left. - M_y^p \left(\frac{\partial^2 \psi_y}{\partial y^2} + \frac{\partial^2 \psi_x}{\partial x \partial y} \right) - P_z \left(\frac{\partial \psi_x}{\partial x} + \frac{\partial \psi_y}{\partial y} \right) \right\} dA, \end{aligned} \tag{16-2}$$

$$\begin{aligned} \Pi_{NC2} = \frac{1}{2} \int_{\Omega} \tau_{ijk}^{(1)} \eta_{ijk}^{(1)} d\Omega = \frac{1}{2} \int_A \left\{ T_{xxx} \frac{\partial^2 u}{\partial x^2} + T_{yyy} \frac{\partial^2 v}{\partial y^2} + T_{zzz} \left(\frac{\partial^2 w}{\partial x^2} - 2 \frac{\partial \psi_x}{\partial x} \right) + T_{xxy} \left(2 \frac{\partial^2 u}{\partial x \partial y} + \frac{\partial^2 v}{\partial x^2} \right) \right. \\ \left. + T_{xyz} \left(2 \frac{\partial^2 w}{\partial x \partial y} - 2 \frac{\partial \psi_x}{\partial y} - 2 \frac{\partial \psi_y}{\partial x} \right) + T_{yyx} \left(\frac{\partial^2 u}{\partial y^2} + 2 \frac{\partial^2 v}{\partial x \partial y} \right) + T_{yyz} \left(\frac{\partial^2 w}{\partial y^2} - 2 \frac{\partial \psi_y}{\partial y} \right) \right. \\ \left. - M_{xxx} \frac{\partial^2 \psi_x}{\partial x^2} - M_{yyy} \frac{\partial^2 \psi_y}{\partial y^2} - M_{xxy} \left(2 \frac{\partial^2 \psi_x}{\partial x \partial y} + \frac{\partial^2 \psi_y}{\partial x^2} \right) - M_{yyx} \left(\frac{\partial^2 \psi_x}{\partial y^2} + 2 \frac{\partial^2 \psi_y}{\partial x \partial y} \right) \right\} dA, \end{aligned} \tag{16-3}$$

$$\begin{aligned} \Pi_{NC3} = \frac{1}{2} \int_{\Omega} m_{ij}^s \chi_{ij}^s d\Omega = \frac{1}{2} \int_A \left\{ \frac{Y_{xx}}{2} \left(\frac{\partial^2 w}{\partial x \partial y} + \frac{\partial \psi_y}{\partial x} \right) - \frac{Y_{yy}}{2} \left(\frac{\partial^2 w}{\partial x \partial y} + \frac{\partial \psi_x}{\partial y} \right) + \frac{Y_{zz}}{2} \left(\frac{\partial \psi_x}{\partial y} - \frac{\partial \psi_y}{\partial x} \right) \right. \\ \left. + \frac{Y_{xy}}{2} \left(\frac{\partial^2 w}{\partial y^2} + \frac{\partial \psi_y}{\partial y} - \frac{\partial^2 w}{\partial x^2} - \frac{\partial \psi_x}{\partial x} \right) + \frac{Y_{xz}}{2} \left(\frac{\partial^2 v}{\partial x^2} - \frac{\partial^2 u}{\partial x \partial y} \right) + \frac{Y_{yz}}{2} \left(\frac{\partial^2 v}{\partial x \partial y} - \frac{\partial^2 u}{\partial y^2} \right) \right. \\ \left. + \frac{H_{xz}}{2} \left(\frac{\partial^2 \psi_x}{\partial x \partial y} - \frac{\partial^2 \psi_y}{\partial x^2} \right) + \frac{H_{yz}}{2} \left(\frac{\partial^2 \psi_x}{\partial y^2} - \frac{\partial^2 \psi_y}{\partial x \partial y} \right) \right\} dA \end{aligned} \tag{16-4}$$

in which A is the surface of midplane of the microplate. The kinetic energy of FG microplate Π_T is given by

$$\Pi_T = \frac{1}{2} \int_A \int_{-\frac{h}{2}}^{\frac{h}{2}} \rho \left[\left(\frac{\partial u_1}{\partial t} \right)^2 + \left(\frac{\partial u_2}{\partial t} \right)^2 + \left(\frac{\partial u_3}{\partial t} \right)^2 \right] dz dA \tag{17}$$

By introducing the inertia terms as $\{I_0, I_1, I_2\} = \int_{-h/2}^{h/2} \rho(z) \{1, z, z^2\} dz$ and substituting the components of displacement from Eq. (3) into the preceding equation we get

$$\Pi_T = \frac{1}{2} \int_A \left[I_0 \left(\frac{\partial u}{\partial t} \right)^2 - 2I_1 \frac{\partial u}{\partial t} \frac{\partial \psi_x}{\partial t} + I_2 \left(\frac{\partial \psi_x}{\partial t} \right)^2 + I_0 \left(\frac{\partial v}{\partial t} \right)^2 - 2I_1 \frac{\partial v}{\partial t} \frac{\partial \psi_y}{\partial t} + I_2 \left(\frac{\partial \psi_y}{\partial t} \right)^2 + I_0 \left(\frac{\partial w}{\partial t} \right)^2 \right] dA \tag{18}$$

The work done by the in-plane prebuckling forces and the transverse load is given by

$$\Pi_w = \frac{1}{2} \int_A \left[N_{xx}^0 \left(\frac{\partial w}{\partial x} \right)^2 + 2N_{xy}^0 \frac{\partial w}{\partial x} \frac{\partial w}{\partial y} + N_{yy}^0 \left(\frac{\partial w}{\partial y} \right)^2 \right] dA - \int_A q(t, x, y) w dA, \tag{19}$$

Now, Hamilton's principle is applied. To this end, the expressions related to the total strain energy, kinetic energy and the work done by the external loads obtained above are first inserted into Eq. (12). Afterward, the variation of u , v , w , ψ_x and ψ_y and integration by parts is taken. Setting the resulting coefficients of δu , δv , δw , $\delta\psi_x$ and $\delta\psi_y$ to zero yields the following governing equations

$$\frac{\partial N_{xx}}{\partial x} + \frac{\partial N_{xy}}{\partial y} + \frac{1}{2} \frac{\partial^2 Y_{xz}}{\partial x \partial y} + \frac{1}{2} \frac{\partial^2 Y_{yz}}{\partial y^2} - \frac{\partial^2 P_x}{\partial x^2} - \frac{\partial^2 P_y}{\partial x \partial y} + \mathcal{H}_1 = I_0 \frac{\partial^2 u}{\partial t^2} - I_1 \frac{\partial^2 \psi_x}{\partial t^2} \tag{20-1}$$

$$\frac{\partial N_{xy}}{\partial x} + \frac{\partial N_{yy}}{\partial y} - \frac{1}{2} \frac{\partial^2 Y_{yz}}{\partial x \partial y} - \frac{1}{2} \frac{\partial^2 Y_{xz}}{\partial x^2} - \frac{\partial^2 P_x}{\partial x \partial y} - \frac{\partial^2 P_y}{\partial y^2} + \mathcal{H}_2 = I_0 \frac{\partial^2 v}{\partial t^2} - I_1 \frac{\partial^2 \psi_y}{\partial t^2} \tag{20-2}$$

$$\begin{aligned} \frac{\partial Q_x}{\partial x} + \frac{\partial Q_y}{\partial y} + \frac{1}{2} \left(\frac{\partial^2 Y_{xy}}{\partial x^2} - \frac{\partial^2 Y_{xx}}{\partial x \partial y} + \frac{\partial^2 Y_{yy}}{\partial x \partial y} - \frac{\partial^2 Y_{xy}}{\partial y^2} \right) \\ + N_{xx}^0 \frac{\partial^2 w}{\partial x^2} + 2N_{xy}^0 \frac{\partial^2 w}{\partial x \partial y} + N_{yy}^0 \frac{\partial^2 w}{\partial x^2} + q + \mathcal{H}_3 = I_0 \frac{\partial^2 w}{\partial t^2} \end{aligned} \tag{20-3}$$

$$Q_x - \frac{\partial M_{xx}}{\partial x} - \frac{\partial M_{xy}}{\partial y} + \frac{1}{2} \left(\frac{\partial Y_{zz}}{\partial y} - \frac{\partial Y_{xy}}{\partial x} - \frac{\partial Y_{yy}}{\partial y} - \frac{\partial^2 H_{xz}}{\partial x \partial y} - \frac{\partial^2 H_{yz}}{\partial y^2} \right) + \mathcal{H}_4 = I_0 \frac{\partial^2 \psi_x}{\partial t^2} - I_1 \frac{\partial^2 u}{\partial t^2} \tag{20-4}$$

$$Q_y - \frac{\partial M_{xy}}{\partial x} - \frac{\partial M_{yy}}{\partial y} + \frac{1}{2} \left(\frac{\partial Y_{xx}}{\partial x} - \frac{\partial Y_{zz}}{\partial x} + \frac{\partial Y_{xy}}{\partial y} + \frac{\partial^2 H_{xz}}{\partial x^2} + \frac{\partial^2 H_{yz}}{\partial x \partial y} \right) + \mathcal{H}_5 = I_0 \frac{\partial^2 \psi_y}{\partial t^2} - I_1 \frac{\partial^2 v}{\partial t^2} \tag{20-5}$$

in which

$$\begin{aligned} \mathcal{H}_1 = - \left(\frac{\partial^2 T_{xxx}}{\partial x^2} + 2 \frac{\partial^2 T_{xy}}{\partial x \partial y} + \frac{\partial^2 T_{yyx}}{\partial y^2} \right), \quad \mathcal{H}_2 = - \left(\frac{\partial^2 T_{xy}}{\partial x^2} + 2 \frac{\partial^2 T_{yyx}}{\partial x \partial y} + \frac{\partial^2 T_{yyy}}{\partial y^2} \right), \\ \mathcal{H}_3 = - \left(\frac{\partial^2 T_{zzz}}{\partial x^2} + 2 \frac{\partial^2 T_{xyz}}{\partial x \partial y} + \frac{\partial^2 T_{yyz}}{\partial y^2} \right), \\ \mathcal{H}_4 = \frac{\partial^2 M_{xxx}}{\partial x^2} + 2 \frac{\partial^2 M_{xy}}{\partial x \partial y} + \frac{\partial^2 M_{yyx}}{\partial y^2} - 2 \frac{\partial T_{xyz}}{\partial y} - 2 \frac{\partial T_{xxx}}{\partial x} - \frac{\partial P_z}{\partial x} + \frac{\partial^2 M_x^p}{\partial x^2} + \frac{\partial^2 M_y^p}{\partial x \partial y}, \\ \mathcal{H}_5 = \frac{\partial^2 M_{xy}}{\partial x^2} + 2 \frac{\partial^2 M_{yyx}}{\partial x \partial y} + \frac{\partial^2 M_{yyy}}{\partial y^2} - 2 \frac{\partial T_{xyz}}{\partial x} - 2 \frac{\partial T_{yyz}}{\partial y} - \frac{\partial P_z}{\partial y} + \frac{\partial^2 M_x^p}{\partial x \partial y} + \frac{\partial^2 M_y^p}{\partial y^2}. \end{aligned} \tag{21}$$

Also, from the variational approach, the corresponding boundary conditions are obtained as

$$\delta u = 0 \quad \text{or} \quad \tilde{N}_{xx} n_x + \tilde{N}_{xy} n_y = 0, \tag{22-1}$$

$$\begin{aligned} \delta\left(\frac{\partial u}{\partial x}\right) &= 0 \text{ or } (P_x + T_{xxx})n_x + \left(\frac{1}{2}P_y + T_{xxy} - \frac{1}{4}Y_{xz}\right)n_y = 0, \\ \delta\left(\frac{\partial u}{\partial y}\right) &= 0 \text{ or } \left(\frac{1}{2}P_y + T_{xxy} - \frac{1}{4}Y_{xz}\right)n_x + \left(T_{yyx} - \frac{1}{2}Y_{yz}\right)n_y = 0, \\ \delta v &= 0 \text{ or } \tilde{N}_{yx}n_x + \tilde{N}_{yy}n_y = 0 \\ \delta\left(\frac{\partial v}{\partial x}\right) &= 0 \text{ or } \left(\frac{1}{2}Y_{xz} + T_{xxy}\right)n_x + \left(\frac{1}{4}Y_{yz} + \frac{1}{2}P_x + T_{yyx}\right)n_y = 0 \\ \delta\left(\frac{\partial v}{\partial y}\right) &= 0 \text{ or } \left(\frac{1}{4}Y_{yz} + \frac{1}{2}P_x + T_{yyx}\right)n_x + (P_y + T_{yyy})n_y = 0 \end{aligned} \quad (22-2)$$

$$\begin{aligned} \delta w &= 0 \text{ or } \tilde{Q}_x n_x + \tilde{Q}_y n_y = 0 \quad \delta\left(\frac{\partial w}{\partial x}\right) = 0 \text{ or } \left(\frac{1}{2}Y_{xy} + T_{zzz}\right)n_x + \left(\frac{Y_{xx} - Y_{yy}}{4} + T_{xyz}\right)n_y = 0 \\ \delta\left(\frac{\partial w}{\partial y}\right) &= 0 \text{ or } \left(\frac{Y_{xx} - Y_{yy}}{4} + T_{xyz}\right)n_x + \left(\frac{1}{2}Y_{xy} + T_{yyz}\right)n_y = 0 \end{aligned} \quad (22-3)$$

$$\begin{aligned} \delta\psi_x &= 0 \text{ or } \tilde{M}_{xx}n_x + \tilde{M}_{xy}n_y = 0 \\ \delta\left(\frac{\partial \psi_x}{\partial x}\right) &= 0 \text{ or } (M_x^p + M_{xxx})n_x + \left(\frac{1}{4}H_{xz} - \frac{1}{2}M_y^p - M_{xxy}\right)n_y = 0 \\ \delta\left(\frac{\partial \psi_x}{\partial y}\right) &= 0 \text{ or } \left(\frac{1}{4}H_{xz} - \frac{1}{2}M_y^p - M_{xxy}\right)n_x + \left(\frac{1}{2}H_{yz} - M_{yyx}\right)n_y = 0 \end{aligned} \quad (22-4)$$

$$\begin{aligned} \delta\psi_y &= 0 \text{ or } \tilde{M}_{yx}n_x + \tilde{M}_{yy}n_y = 0 \\ \delta\left(\frac{\partial \psi_y}{\partial x}\right) &= 0 \text{ or } \left(\frac{1}{2}H_{xz} + M_{xxy}\right)n_x + \left(\frac{1}{4}H_{yz} + \frac{1}{2}M_x^p + M_{yyx}\right)n_y = 0 \\ \delta\left(\frac{\partial \psi_y}{\partial y}\right) &= 0 \text{ or } \left(\frac{1}{4}H_{yz} + \frac{1}{2}M_x^p + M_{yyx}\right)n_x + (M_y^p + M_{yyy})n_y = 0 \end{aligned} \quad (22-5)$$

where n_x and n_y are the unit base vectors along the x- and y-axes, respectively. The elements \tilde{N}_{ij} , \tilde{M}_{ij} and \tilde{Q}_j ; ($i, j = x, y$) are given in Appendix.

By means of Eqs. (22), the boundary conditions related to simply supported (S) and clamped (C) edges are obtained as follows

A. Clamped boundary condition

At $x = 0, a$:

$$u = u_{,x} = v = v_{,x} = w = w_{,x} = \psi_x = \psi_{x,x} = \psi_y = \psi_{y,x} = 0 \quad (23-1)$$

At $y = 0, b$:

$$u = u_{,y} = v = v_{,y} = w = w_{,y} = \psi_x = \psi_{x,y} = \psi_y = \psi_{y,y} = 0 \tag{23-2}$$

B. Simply supported boundary condition

At $x = 0, a$:

$$u = u_{,x} = v = \frac{1}{2} Y_{xz} + T_{xxy} = w = \frac{1}{2} Y_{xy} - T_{zzz} = 0$$

$$M_{xx} + \frac{2Y_{xy} + H_{xz,y}}{4} + P_z - \frac{2M_{x,x}^p + M_{y,y}^p}{2} + 2T_{zzz} - M_{xxx,x} - M_{xyy,y} = \psi_{x,x} = 0 \tag{23-3}$$

$$M_{xy} + \frac{Y_{zz} - Y_{xx}}{2} - \frac{2H_{xz,x} + H_{yz,y}}{4} - M_{xxy,x} + 2T_{xyz} - \frac{1}{2} M_{x,y}^p - M_{yyx,y} = \frac{1}{2} H_{xz} + M_{xxy} = 0$$

At $y = 0, b$:

$$u = \frac{1}{2} Y_{yz} - T_{yyx} = v = v_{,y} = w = \frac{1}{2} Y_{xy} + T_{yyz} = 0$$

$$M_{xy} + \frac{Y_{yy} - Y_{zz}}{2} + \frac{2H_{yz,y} + H_{xz,x}}{4} + 2T_{xyz} - \frac{1}{2} M_{y,x}^p - M_{yyx,x} - M_{xxy,x} = -\frac{1}{2} H_{yz} + M_{yyx} = 0 \tag{23-4}$$

$$M_{yy} - M_{y,y}^p + P_z - \frac{1}{2} Y_{xy} + 2T_{yyz} - M_{yyy,y} - \frac{1}{4} H_{yz,x} - \frac{1}{2} M_{x,x}^p - M_{yyx,x} = \psi_{y,y} = 0$$

where “,” denotes the differentiation. With various combinations of simply supported and clamped edges, one can derive different types of end conditions for the FG rectangular microplate.

As stated at first, the size-dependent governing equations and edge conditions reduce to those of classical theory when all the material length scale parameters l_0, l_1, l_2 vanish. Also, one can get the ones for an FG Reissner–Mindlin microplate modeled by the modified couple stress theory by setting l_0 and l_1 to zero. Moreover, the present governing equations and edge conditions will decline into those of the FG Timoshenko microbeam, if the components of displacement v, ψ_y and the terms relevant to the derivations with respect to y neglect.

The stiffness components $(A_{ij}, B_{ij}, D_{ij}, i = 1, 5, j = 1, 2, 5)$ and the non-dimensional parameters are defined as

$$\{A_{11}, B_{11}, D_{11}\} = \int_{-h/2}^{h/2} (\lambda(z) + 2\mu(z)) \{1, z, z^2\} dz, \quad \{A_{12}, B_{12}, D_{12}\} = \int_{-h/2}^{h/2} \lambda(z) \{1, z, z^2\} dz, \tag{24}$$

$$\{A_{55}, B_{55}, D_{55}\} = \int_{-h/2}^{h/2} \mu(z) \{1, z, z^2\} dz,$$

$$\xi = \frac{x}{a}, \zeta = \frac{y}{b}, (\bar{u}, \bar{v}, \bar{w}, \bar{\psi}_x, \bar{\psi}_y) = \left(\frac{u}{h}, \frac{v}{h}, \frac{w}{h}, \psi_x, \psi_y \right), (\bar{I}_0, \bar{I}_1, \bar{I}_2) = \left(\frac{I_0}{I_{00}}, \frac{I_1}{I_{00}h}, \frac{I_2}{I_{00}h^2} \right)$$

$$(a_{11}, a_{12}, a_{55}) = \left(\frac{A_{11}}{A_{110}}, \frac{A_{12}}{A_{110}}, \frac{A_{55}}{A_{110}} \right), (b_{11}, b_{12}, b_{55}) = \left(\frac{B_{11}}{A_{110}h}, \frac{B_{12}}{A_{110}h}, \frac{B_{55}}{A_{110}h} \right)$$

$$(d_{11}, d_{12}, d_{55}) = \left(\frac{D_{11}}{A_{110}h^2}, \frac{D_{12}}{A_{110}h^2}, \frac{D_{55}}{A_{110}h^2} \right), (\eta_1, \eta_2) = \left(\frac{a}{h}, \frac{b}{h} \right), \kappa = \frac{a}{b},$$

$$(l_0, l_1, l_2) = \frac{(l_0, l_1, l_2)}{h}, \tau = \frac{t}{a} \sqrt{\frac{A_{110}}{I_{00}}}, (\bar{N}_{xx}^0, \bar{N}_{yy}^0, \bar{N}_{xy}^0) = \left(\frac{N_{xx}^0}{A_{110}}, \frac{N_{yy}^0}{A_{110}}, \frac{N_{xy}^0}{A_{110}} \right), \bar{N}_T = \frac{N_T}{A_{110}}, \bar{q} = \frac{qa^2}{hA_{110}}$$
(25)

respectively, where I_{00}, A_{110} are the values of I_0 and A_{11} corresponding to a homogeneous metal microplate.

On substitution of the resultant forces and moments given in Eqs. (14) and (15) in terms of displacement into Eqs. (20) and using the relationships (25), one can achieve

$$a_{11} \frac{\partial^2 \bar{u}}{\partial \xi^2} + a_{55} \kappa^2 \frac{\partial^2 \bar{u}}{\partial \zeta^2} + (a_{12} + a_{55}) \kappa \frac{\partial^2 \bar{v}}{\partial \zeta \partial \xi} + b_{11} \frac{\partial^2 \bar{\psi}_x}{\partial \xi^2} + b_{55} \kappa^2 \frac{\partial^2 \bar{\psi}_x}{\partial \zeta^2} + (b_{12} + b_{55}) \kappa \frac{\partial^2 \bar{\psi}_y}{\partial \zeta \partial \xi}$$

$$- \frac{c_1}{\eta_1^2} \left(a_{55} \frac{\partial^4 \bar{u}}{\partial \xi^4} + b_{55} \frac{\partial^4 \bar{\psi}_x}{\partial \xi^4} \right) - \frac{c_2 \kappa^4}{\eta_1^2} \left(a_{55} \frac{\partial^4 \bar{u}}{\partial \zeta^4} + b_{55} \frac{\partial^4 \bar{\psi}_x}{\partial \zeta^4} \right) - \frac{c_3 \kappa^2}{\eta_1^2} \left(a_{55} \frac{\partial^4 \bar{u}}{\partial \xi^2 \partial \zeta^2} + b_{55} \frac{\partial^4 \bar{\psi}_x}{\partial \xi^2 \partial \zeta^2} \right)$$

$$- \frac{a_{55} c_4 \kappa}{\eta_1^2} \left(\frac{\partial^4 \bar{v}}{\partial \zeta \partial \xi^3} + \kappa^2 \frac{\partial^4 \bar{v}}{\partial \zeta^3 \partial \xi} \right) - \frac{b_{55} c_4 \kappa}{\eta_1^2} \left(\frac{\partial^4 \bar{\psi}_y}{\partial \zeta \partial \xi^3} + \kappa^2 \frac{\partial^4 \bar{\psi}_y}{\partial \zeta^3 \partial \xi} \right) = \bar{I}_0 \frac{\partial^2 \bar{u}}{\partial \tau^2} + \bar{I}_1 \frac{\partial^2 \bar{\psi}_x}{\partial \tau^2},$$
(26-1)

$$(a_{12} + a_{55}) \kappa \frac{\partial^2 \bar{u}}{\partial \zeta \partial \xi} + a_{11} \kappa^2 \frac{\partial^2 \bar{v}}{\partial \zeta^2} + a_{55} \frac{\partial^2 \bar{v}}{\partial \xi^2} + (b_{12} + b_{55}) \kappa \frac{\partial^2 \bar{\psi}_x}{\partial \zeta \partial \xi} + b_{11} \kappa^2 \frac{\partial^2 \bar{\psi}_y}{\partial \zeta^2} + b_{55} \frac{\partial^2 \bar{\psi}_y}{\partial \xi^2}$$

$$- \frac{c_1 \kappa^4}{\eta_1^2} \left(a_{55} \frac{\partial^4 \bar{v}}{\partial \zeta^4} + b_{55} \frac{\partial^4 \bar{\psi}_y}{\partial \zeta^4} \right) - \frac{c_2}{\eta_1^2} \left(a_{55} \frac{\partial^4 \bar{v}}{\partial \xi^4} + b_{55} \frac{\partial^4 \bar{\psi}_y}{\partial \xi^4} \right) - \frac{c_3 \kappa^2}{\eta_1^2} \left(a_{55} \frac{\partial^4 \bar{v}}{\partial \zeta^2 \partial \xi^2} + b_{55} \frac{\partial^4 \bar{\psi}_y}{\partial \zeta^2 \partial \xi^2} \right)$$

$$- \frac{a_{55} c_4 \kappa}{\eta_1^2} \left(\frac{\partial^4 \bar{u}}{\partial \zeta \partial \xi^3} + \kappa^2 \frac{\partial^4 \bar{u}}{\partial \zeta^3 \partial \xi} \right) - \frac{b_{55} c_4 \kappa}{\eta_1^2} \left(\frac{\partial^4 \bar{\psi}_x}{\partial \zeta \partial \xi^3} + \kappa^2 \frac{\partial^4 \bar{\psi}_x}{\partial \zeta^3 \partial \xi} \right) = \bar{I}_0 \frac{\partial^2 \bar{v}}{\partial \tau^2} + \bar{I}_1 \frac{\partial^2 \bar{\psi}_y}{\partial \tau^2},$$
(26-2)

$$k_s a_{55} \left(\frac{\partial^2 \bar{w}}{\partial \xi^2} + \kappa^2 \frac{\partial^2 \bar{w}}{\partial \zeta^2} + \eta_1 \frac{\partial \bar{\psi}_x}{\partial \xi} + \kappa \eta_1 \frac{\partial \bar{\psi}_y}{\partial \zeta} \right) - \frac{a_{55} c_5}{\eta_1} \left(\frac{\partial^3 \bar{\psi}_x}{\partial \xi^3} + \kappa^2 \frac{\partial^3 \bar{\psi}_x}{\partial \zeta^2 \partial \xi} + \kappa \frac{\partial^3 \bar{\psi}_y}{\partial \zeta \partial \xi^2} + \kappa^3 \frac{\partial^3 \bar{\psi}_y}{\partial \zeta^3} \right)$$

$$- \frac{a_{55} c_2}{\eta_1^2} \left(\frac{\partial^4 \bar{w}}{\partial \xi^4} + 2\kappa^2 \frac{\partial^4 \bar{w}}{\partial \zeta^2 \partial \xi^2} + \kappa^4 \frac{\partial^4 \bar{w}}{\partial \zeta^4} \right) + \bar{N}_{xx}^0 \frac{\partial^2 \bar{w}}{\partial \xi^2} + 2\kappa \bar{N}_{xy}^0 \frac{\partial^2 \bar{w}}{\partial \zeta \partial \xi} + \kappa^2 \bar{N}_{yy}^0 \frac{\partial^2 \bar{w}}{\partial \zeta^2} - \bar{N}_T \left(\frac{\partial^2 \bar{w}}{\partial \xi^2} + \kappa^2 \frac{\partial^2 \bar{w}}{\partial \zeta^2} \right) + \bar{q} = \bar{I}_0 \frac{\partial^2 \bar{w}}{\partial \tau^2},$$
(26-3)

$$\begin{aligned}
 & b_{11} \frac{\partial^2 \bar{u}}{\partial \xi^2} + b_{55} \kappa^2 \frac{\partial^2 \bar{u}}{\partial \zeta^2} + (b_{12} + b_{55}) \kappa \frac{\partial^2 \bar{v}}{\partial \zeta \partial \xi} + d_{11} \frac{\partial^2 \bar{\psi}_x}{\partial \xi^2} + d_{55} \kappa^2 \frac{\partial^2 \bar{\psi}_x}{\partial \zeta^2} + (d_{12} + d_{55}) \kappa \frac{\partial^2 \bar{\psi}_y}{\partial \zeta \partial \xi} \\
 & - k_s a_{55} \eta_{II} \left(\eta_{II} \bar{\psi}_x + \frac{\partial \bar{w}}{\partial \xi} \right) - \frac{c_1}{\eta_1^2} \left(b_{55} \frac{\partial^4 \bar{u}}{\partial \xi^4} + d_{55} \frac{\partial^4 \bar{\psi}_x}{\partial \xi^4} \right) - \frac{c_2 \kappa^4}{\eta_1^2} \left(b_{55} \frac{\partial^4 \bar{u}}{\partial \zeta^4} + d_{55} \frac{\partial^4 \bar{\psi}_x}{\partial \zeta^4} \right) \\
 & - \frac{c_3 \kappa^2}{\eta_1^2} \left(b_{55} \frac{\partial^4 \bar{u}}{\partial \xi^2 \partial \zeta^2} + d_{55} \frac{\partial^4 \bar{\psi}_x}{\partial \xi^2 \partial \zeta^2} \right) - \frac{b_{55} c_4 \kappa}{\eta_1^2} \left(\frac{\partial^4 \bar{v}}{\partial \xi^3 \partial \zeta} + \kappa^2 \frac{\partial^4 \bar{v}}{\partial \zeta \partial \xi^3} \right) - \frac{d_{55} c_4 \kappa}{\eta_1^2} \left(\frac{\partial^4 \bar{\psi}_y}{\partial \xi^3 \partial \zeta} + \kappa^2 \frac{\partial^4 \bar{\psi}_y}{\partial \zeta \partial \xi^3} \right) \\
 & + \frac{a_{55} c_5}{\eta_1} \left(\frac{\partial^3 \bar{w}}{\partial \xi^3} + \kappa^2 \frac{\partial^3 \bar{w}}{\partial \zeta^3 \partial \xi} \right) + a_{55} c_6 \left(\frac{\partial^2 \bar{\psi}_x}{\partial \xi^2} + \kappa^2 \frac{\partial^2 \bar{\psi}_x}{\partial \zeta^2} \right) + a_{55} c_7 \kappa \left(\frac{\partial^2 \bar{\psi}_y}{\partial \zeta \partial \xi} - \kappa \frac{\partial^2 \bar{\psi}_x}{\partial \zeta^2} \right) = \bar{I}_2 \frac{\partial^2 \bar{\psi}_x}{\partial \tau^2} + \bar{I}_1 \frac{\partial^2 \bar{u}}{\partial \tau^2},
 \end{aligned} \tag{26-4}$$

$$\begin{aligned}
 & (b_{12} + b_{55}) \kappa \frac{\partial^2 \bar{u}}{\partial \zeta \partial \xi} + b_{11} \kappa^2 \frac{\partial^2 \bar{v}}{\partial \zeta^2} + b_{55} \frac{\partial^2 \bar{v}}{\partial \xi^2} + (d_{12} + d_{55}) \kappa \frac{\partial^2 \bar{\psi}_x}{\partial \zeta \partial \xi} + d_{11} \kappa^2 \frac{\partial^2 \bar{\psi}_y}{\partial \zeta^2} + d_{55} \frac{\partial^2 \bar{\psi}_y}{\partial \xi^2} \\
 & - k_s a_{55} \eta_{II} \left(\eta_{II} \bar{\psi}_y + \kappa \frac{\partial \bar{w}}{\partial \zeta} \right) - \frac{c_1 \kappa^4}{\eta_1^2} \left(b_{55} \frac{\partial^4 \bar{v}}{\partial \zeta^4} + d_{55} \frac{\partial^4 \bar{\psi}_y}{\partial \zeta^4} \right) - \frac{c_2}{\eta_1^2} \left(b_{55} \frac{\partial^4 \bar{v}}{\partial \xi^4} + d_{55} \frac{\partial^4 \bar{\psi}_y}{\partial \xi^4} \right) \\
 & - \frac{c_3 \kappa^2}{\eta_1^2} \left(b_{55} \frac{\partial^4 \bar{v}}{\partial \xi^2 \partial \zeta^2} + d_{55} \frac{\partial^4 \bar{\psi}_y}{\partial \xi^2 \partial \zeta^2} \right) - \frac{b_{55} c_4 \kappa}{\eta_1^2} \left(\frac{\partial^4 \bar{u}}{\partial \zeta \partial \xi^3} + \kappa^2 \frac{\partial^4 \bar{u}}{\partial \xi^3 \partial \zeta} \right) - \frac{d_{55} c_4 \kappa}{\eta_1^2} \left(\frac{\partial^4 \bar{\psi}_x}{\partial \zeta \partial \xi^3} + \kappa^2 \frac{\partial^4 \bar{\psi}_x}{\partial \xi^3 \partial \zeta} \right) \\
 & + \frac{a_{55} c_5 \kappa}{\eta_1} \left(\frac{\partial^3 \bar{w}}{\partial \zeta \partial \xi^2} + \kappa^2 \frac{\partial^3 \bar{w}}{\partial \xi^3} \right) + a_{55} c_6 \left(\frac{\partial^2 \bar{\psi}_y}{\partial \xi^2} + \kappa^2 \frac{\partial^2 \bar{\psi}_y}{\partial \zeta^2} \right) + a_{55} c_7 \left(\kappa \frac{\partial^2 \bar{\psi}_x}{\partial \zeta \partial \xi} - \frac{\partial^2 \bar{\psi}_y}{\partial \xi^2} \right) = \bar{I}_2 \frac{\partial^2 \bar{\psi}_y}{\partial \tau^2} + \bar{I}_1 \frac{\partial^2 \bar{v}}{\partial \tau^2}.
 \end{aligned} \tag{26-5}$$

in which the following quantities are used

$$\begin{aligned}
 c_1 &= \left(2\ell_0^2 + \frac{4}{5} \ell_1^2 \right), c_2 = \left(\frac{8}{15} \ell_1^2 + \frac{1}{4} \ell_2^2 \right), c_3 = \left(2\ell_0^2 + \frac{4}{3} \ell_1^2 + \frac{1}{4} \ell_2^2 \right), c_4 = \left(2\ell_0^2 + \frac{4}{15} \ell_1^2 - \frac{1}{4} \ell_2^2 \right), \\
 c_5 &= \left(\frac{16}{15} \ell_1^2 - \frac{1}{4} \ell_2^2 \right), c_6 = \left(2\ell_0^2 + \frac{32}{15} \ell_1^2 + \frac{1}{4} \ell_2^2 \right), c_7 = \left(2\ell_0^2 + \frac{4}{5} \ell_1^2 - \frac{3}{4} \ell_2^2 \right).
 \end{aligned} \tag{27}$$

2.5 Thermal Loading

Thermal load is considered as

$$N_T = \int_{-h/2}^{h/2} \frac{E(z) \alpha(z) T(z)}{1 - \nu(z)} dz, \tag{28}$$

The one dimensional steady-state heat transfer equation through the plate thickness is given by

$$\frac{d}{dz} \left[K(z) \frac{dT}{dz} \right] = 0, \quad T = \begin{cases} T_m & z = -\frac{h}{2} \\ T_c & z = +\frac{h}{2} \end{cases} \tag{29}$$

where T_c and T_m are the temperatures at the ceramic side and the metal side, respectively. Inserting $K(z)$ from Eq. (1) into Eq. (29), the solution of Eq. (29) gives the temperature distribution as

$$T(z) = \frac{\Delta T}{\int_{-h/2}^z \frac{dz}{K(z)}} \int_{-h/2}^z \frac{dz}{K(z)} + T_m, \quad \Delta T = T_c - T_m \tag{30}$$

For linear temperature distribution across the thickness we have

$$T(z) = \frac{\Delta T}{h} \left(z + \frac{h}{2} \right) + T_m \tag{31}$$

3 DISCRETIZATION AND SOLUTION OF GOVERNING EQUATIONS

To solve the governing equations, the generalized differential quadrature method as a powerful numerical technique is adopted to transform the equations of motion and boundary conditions into discrete forms. When discretizing the problem, the grid point distributions in the ξ - and ζ - directions with N and M nodes, respectively are located at the shifted Chebyshev–Gauss–Lobatto as

$$\xi_i = \frac{1}{2a} \left(1 - \cos \frac{i-1}{N-1} \pi \right); \quad i = 1 : N, \quad \zeta_j = \frac{1}{2b} \left(1 - \cos \frac{j-1}{M-1} \pi \right); \quad j = 1 : M. \tag{32}$$

If the mode shapes of the microplate denote by $\mathbf{U}(\xi, \zeta)$, $\mathbf{V}(\xi, \zeta)$, $\mathbf{W}(\xi, \zeta)$, $\mathbf{\Psi}_x(\xi, \zeta)$, and $\mathbf{\Psi}_y(\xi, \zeta)$ in the domain defined by the vectors $\boldsymbol{\xi}$ and $\boldsymbol{\zeta}$, they can be stated as follows

$$\mathbf{U} = \begin{bmatrix} \bar{u}(\xi_1, \zeta_1) & \bar{u}(\xi_1, \zeta_2) & \dots & \bar{u}(\xi_1, \zeta_M) \\ \bar{u}(\xi_2, \zeta_1) & \bar{u}(\xi_2, \zeta_2) & \dots & \bar{u}(\xi_2, \zeta_M) \\ \vdots & \vdots & \ddots & \vdots \\ \bar{u}(\xi_N, \zeta_1) & \bar{u}(\xi_N, \zeta_2) & \dots & \bar{u}(\xi_N, \zeta_M) \end{bmatrix}, \quad \mathbf{V} = \begin{bmatrix} \bar{v}(\xi_1, \zeta_1) & \bar{v}(\xi_1, \zeta_2) & \dots & \bar{v}(\xi_1, \zeta_M) \\ \bar{v}(\xi_2, \zeta_1) & \bar{v}(\xi_2, \zeta_2) & \dots & \bar{v}(\xi_2, \zeta_M) \\ \vdots & \vdots & \ddots & \vdots \\ \bar{v}(\xi_N, \zeta_1) & \bar{v}(\xi_N, \zeta_2) & \dots & \bar{v}(\xi_N, \zeta_M) \end{bmatrix}, \tag{33}$$

$$\mathbf{W} = \begin{bmatrix} \bar{w}(\xi_1, \zeta_1) & \bar{w}(\xi_1, \zeta_2) & \dots & \bar{w}(\xi_1, \zeta_M) \\ \bar{w}(\xi_2, \zeta_1) & \bar{w}(\xi_2, \zeta_2) & \dots & \bar{w}(\xi_2, \zeta_M) \\ \vdots & \vdots & \ddots & \vdots \\ \bar{w}(\xi_N, \zeta_1) & \bar{w}(\xi_N, \zeta_2) & \dots & \bar{w}(\xi_N, \zeta_M) \end{bmatrix}, \quad \mathbf{\Psi}_x = \begin{bmatrix} \bar{\psi}_x(\xi_1, \zeta_1) & \bar{\psi}_x(\xi_1, \zeta_2) & \dots & \bar{\psi}_x(\xi_1, \zeta_M) \\ \bar{\psi}_x(\xi_2, \zeta_1) & \bar{\psi}_x(\xi_2, \zeta_2) & \dots & \bar{\psi}_x(\xi_2, \zeta_M) \\ \vdots & \vdots & \ddots & \vdots \\ \bar{\psi}_x(\xi_N, \zeta_1) & \bar{\psi}_x(\xi_N, \zeta_2) & \dots & \bar{\psi}_x(\xi_N, \zeta_M) \end{bmatrix},$$

$$\Psi_y = \begin{bmatrix} \bar{\psi}_y(\xi_1, \zeta_1) & \bar{\psi}_y(\xi_1, \zeta_2) & \dots & \bar{\psi}_y(\xi_1, \zeta_M) \\ \bar{\psi}_y(\xi_2, \zeta_1) & \bar{\psi}_y(\xi_2, \zeta_2) & \dots & \bar{\psi}_y(\xi_2, \zeta_M) \\ \vdots & \vdots & \ddots & \vdots \\ \bar{\psi}_y(\xi_N, \zeta_1) & \bar{\psi}_y(\xi_N, \zeta_2) & \dots & \bar{\psi}_y(\xi_N, \zeta_M) \end{bmatrix}$$

The above matrices can be expressed in a column vector form as

$$\begin{aligned} \bar{\mathbf{U}} &= \text{vec}\left(\bar{u}\left(\xi_i, \zeta_j\right)\right), \quad \bar{\mathbf{V}} = \text{vec}\left(\bar{v}\left(\xi_i, \zeta_j\right)\right), \quad \bar{\mathbf{W}} = \text{vec}\left(\bar{w}\left(\xi_i, \zeta_j\right)\right), \\ \bar{\Psi}_x &= \text{vec}\left(\bar{\psi}_x\left(\xi_i, \zeta_j\right)\right), \quad \bar{\Psi}_y = \text{vec}\left(\bar{\psi}_y\left(\xi_i, \zeta_j\right)\right) \quad i=1 \dots N, \quad j=1 \dots M \end{aligned} \tag{34}$$

Note that the forgoing vectors are $NM \times 1$. For a two variable function, the GDQ method can be used to approximate the first or higher order partial derivatives of it, e.g., the second order partial derivative of $U(\xi, \zeta)$ with respect to ξ and ζ is given by

$$\frac{\partial^2 U(\xi, \zeta)}{\partial \xi \partial \zeta} = \left(\mathbf{D}_\zeta^{(1)} \otimes \mathbf{D}_\xi^{(1)}\right) \bar{\mathbf{U}} \tag{35}$$

in which $\mathbf{D}_\zeta^{(1)}$ and $\mathbf{D}_\xi^{(1)}$ represent the weighting coefficients of the first order derivative in the ζ and ξ directions, respectively in GDQ (Ansari et al. (2013)) and \otimes denotes the Kronecker tensor product.

3.1 Bending of FG Microplate

To derive the discrete form of the equations of motion governing the static bending of the microplate, the microplate is considered to be just subjected to the uniformly distributed load. So, the time-dependent and the in-plane prebuckling force terms appeared in the governing equations are first neglected. Then, taking the partial derivatives based on Eq. (35), the governing equations given in Eqs. (26) can be discretized in a shortened form as follows

$$\mathbf{KX} + \mathbf{q} = \mathbf{0} \tag{36}$$

where $\mathbf{X} = \left\{ \bar{\mathbf{U}}^T, \bar{\mathbf{V}}^T, \bar{\mathbf{W}}^T, \bar{\Psi}_x^T, \bar{\Psi}_y^T \right\}^T$. The elements of the stiffness matrix \mathbf{K} and the transverse force vector \mathbf{q} are given in Appendix. The boundary conditions are transformed into the discrete forms in a similar manner. After substituting all the end conditions into Eq. (36), the mode shapes are obtained as

$$\mathbf{X} = \mathbf{K}^{-1} \mathbf{q} \tag{37}$$

3.2 Buckling of FG Microplate

In this section, the microplate is considered to be under the biaxial in-plane prebuckling forces only, (i.e., $\bar{N}_{xx}^0 = \bar{N}_{yy}^0 = P$, $\bar{N}_{xy}^0 = 0$) according to which the transverse load is taken as zero and the time-dependent terms are dropped in the governing equations. Therefore, using Eq. (35), the governing equations (26) can be discretized leading to an eigenvalue problem as

$$\mathbf{KX} + P\mathbf{NX} = 0 \quad (38)$$

The components of the matrix \mathbf{N} are presented in Appendix. The end conditions are imposed by inserting the discrete counterparts of all the boundary conditions into Eqs. (38). Separating the domain and boundary grid points denoted by the subscripts \mathbf{b} and \mathbf{d} respectively, from each other cause the column displacement vector \mathbf{X} to be decomposed as

$$\mathbf{X}_d = \left\{ (\bar{\mathbf{W}})_d^T, (\bar{\Psi}_x)_d^T, (\bar{\Psi}_y)_d^T \right\}^T, \quad \mathbf{X}_b = \left\{ (\bar{\mathbf{W}})_b^T, (\bar{\Psi}_x)_b^T, (\bar{\Psi}_y)_b^T \right\}^T \quad (39)$$

Using the preceding relationship, Eq. (38) can be recast to the standard form of an eigenvalue problem in the domain as

$$\left(\mathbf{K}_{dd} - \mathbf{K}_{db} \mathbf{K}_{bb}^{-1} \mathbf{K}_{bd} \right) \mathbf{X}_d = -P \left(\mathbf{N}_{dd} - \mathbf{N}_{db} \mathbf{K}_{bb}^{-1} \mathbf{K}_{bd} \right) \mathbf{X}_d \quad (40)$$

Also, from this manipulation, the displacement vector corresponding to the boundary grid points is obtained as follows

$$\mathbf{X}_b = -\mathbf{K}_{bb}^{-1} \mathbf{K}_{bd} \mathbf{X}_d \quad (41)$$

By means of two last equations, one can obtain the critical buckling loads and the corresponding buckling mode shapes of the microplate.

3.3 Free Vibration of FG Microplate

In the case of free vibration of the microplate, the components of the displacement are taken to be of the following form

$$\begin{aligned} u(\xi, \zeta, \tau) &= U(\xi, \zeta) e^{i\omega\tau}, \quad v(\xi, \zeta, \tau) = V(\xi, \zeta) e^{i\omega\tau}, \quad w(\xi, \zeta, \tau) = W(\xi, \zeta) e^{i\omega\tau}, \\ \psi_x(\xi, \zeta, \tau) &= \Psi_x(\xi, \zeta) e^{i\omega\tau}, \quad \psi_y(\xi, \zeta, \tau) = \Psi_y(\xi, \zeta) e^{i\omega\tau}. \end{aligned} \quad (42)$$

where ω is the non-dimensional natural frequency. With assumption of $\bar{N}_{xx}^0 = \bar{N}_{yy}^0 = \bar{N}_{xy}^0 = q = 0$, substituting Eqs. (42) into Eqs. (26) and taking the partial derivatives in accordance with relationship (36) yield a condensed discrete form of governing equations as

$$\mathbf{KX} = -\omega^2 \mathbf{MX} \quad (43)$$

where \mathbf{M} is the mass matrix whose components are given in Appendix. By retracing all the steps of the previous section, the natural frequencies and the associated mode shapes of the FG microplate can be acquired.

4 RESULTS AND DISCUSSION

In what follows, the selected numerical results are given to describe the bending, buckling and free vibration behavior of the FG microplate with different edge supports. The results from classical, couple stress and strain gradient theories are presented to make a comparison among the responses predicted by the different theories. In this paper, four commonly-used boundary conditions for a FG microplate is considered which are as follows

1. CCCC: All edges clamped,
2. SSSS: All edges simply supported,
3. CSCS: Two edges along the x direction clamped, remaining ones simply supported,
4. SCSC: Two edges along the x direction simply supported, remaining ones clamped.

The metal and ceramic constituents of the FG microplate are considered to be Aluminum and Silicon Carbide, respectively with the material properties as $E_m=70$ GPa, $\rho_m=2702$ kg/m³, $\nu_m=0.3$, $\alpha_m=22.5 \times 10^{-6}$ K⁻¹, $E_c=427$ GPa, $\rho_c=3100$ kg/m³, $\nu_c=0.17$, $\alpha_c=4 \times 10^{-6}$ K⁻¹. It should be pointed out that no experimental data on the values of the scale parameters corresponding to the FG microplate is available in the open literature. Lam et al (2003) obtained the size scale constant for an isotropic homogenous microbeam as $l=17.6 \mu\text{m}$. Here, the values of the length scale parameters for the FG microplate are approximated by $l=15 \mu\text{m}$ (Sahmani and Ansari (2012)). In the following, the effects of different quantities on the on the response of the FG microplate are delineated.

4.1 Size Scale Effects

Fig. 2 shows the variation of non-dimensional deflection of the FG microplate (maximum deflection of the microplate to its thickness ratio) with non-dimensional size scale (h/l) for the considered three theories. It is noted that the deflection of the microplate corresponding to the CT remains unchanged due to having no length scale constant, whereas it goes up nonlinearly for MCST and MSGT as the size scale increases. It is also observed that the difference between the classical and the non-classical theories is higher for the strain gradient theory. In other words, the size-dependence of MSGT is heavier than MCST especially when the thickness of the microplate is comparable with the length scale parameter. It is attributed to the fact the strain gradient theory incorporates the three strain gradient tensors namely the symmetric rotation gradient tensor, dilatation gradient tensor and the deviatoric stretch gradient tensor, whereas the couple stress theory includes only the symmetric rotation gradient tensor. Further, it is seen that as the size scale increases, the curves converge i.e., the non-classical theories tend to the classical one. In other words, for large-sized structure, the classical theory is able to predict the bending response of the FG microplate.

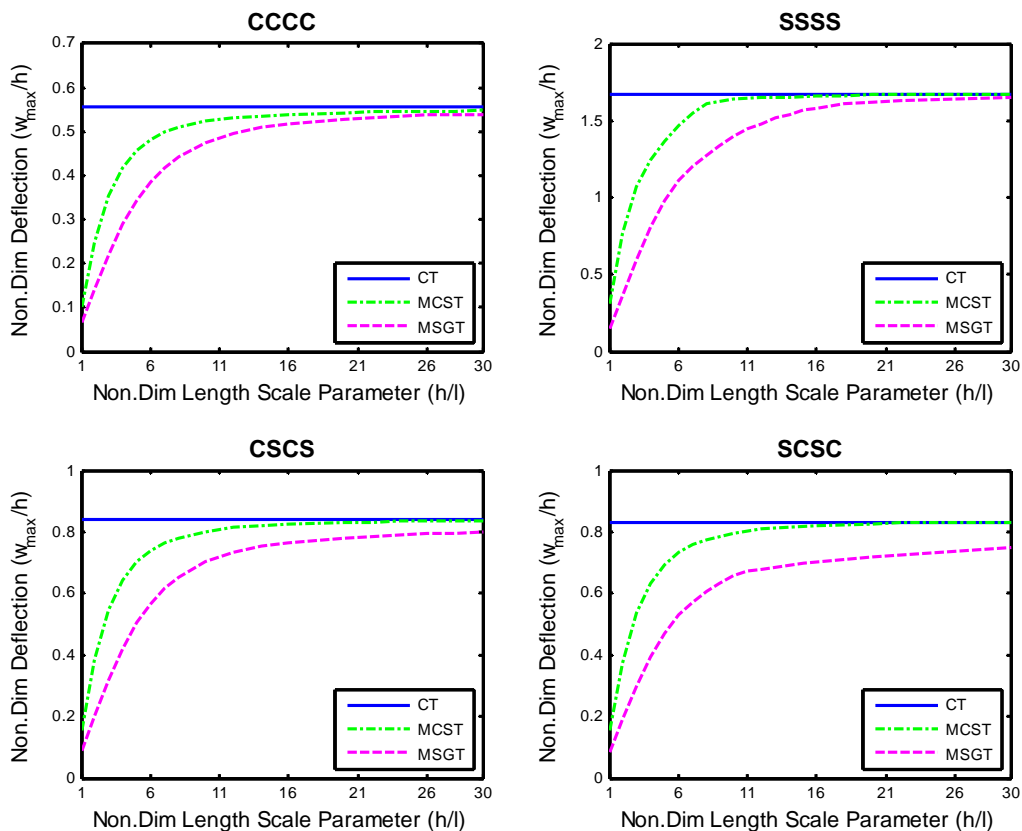


Figure 2: Non-dimensional deflection of FG microplate as a function of non-dimensional length scale parameter predicted by CT, MCST and MSGT with $a/h=10$ and $k_{FGM}=0.2$.

Presented in Fig. 3 is the non-dimensional critical buckling load of the FG microplate as a function of non-dimensional size scale. From this figure one can see that with the increase of the scale constant, the buckling load decreases for the non-classical theories whereas, the load corresponding to the CT keeps constant. In contrast with the results of the previous figure, it is seen that the couple stress and the strain gradient theories predict the buckling load larger than that of the classical theory and this pattern is more evident for the small length scale. From this comparison, it is found that the inclusion of the size scale effect leads to the increase of the stiffness of the microplate. Also, the strain gradient theory is found to predict the buckling load higher than the couple stress theory does due to the incorporation of the more strain gradient tensors which then clarifies the more prominent size-dependence of this theory. Furthermore, it is noted that by increasing the size scale, the gap between the curves associated with the various theories diminishes. It means that as the structural size reduces, the scale effects become more prominent.

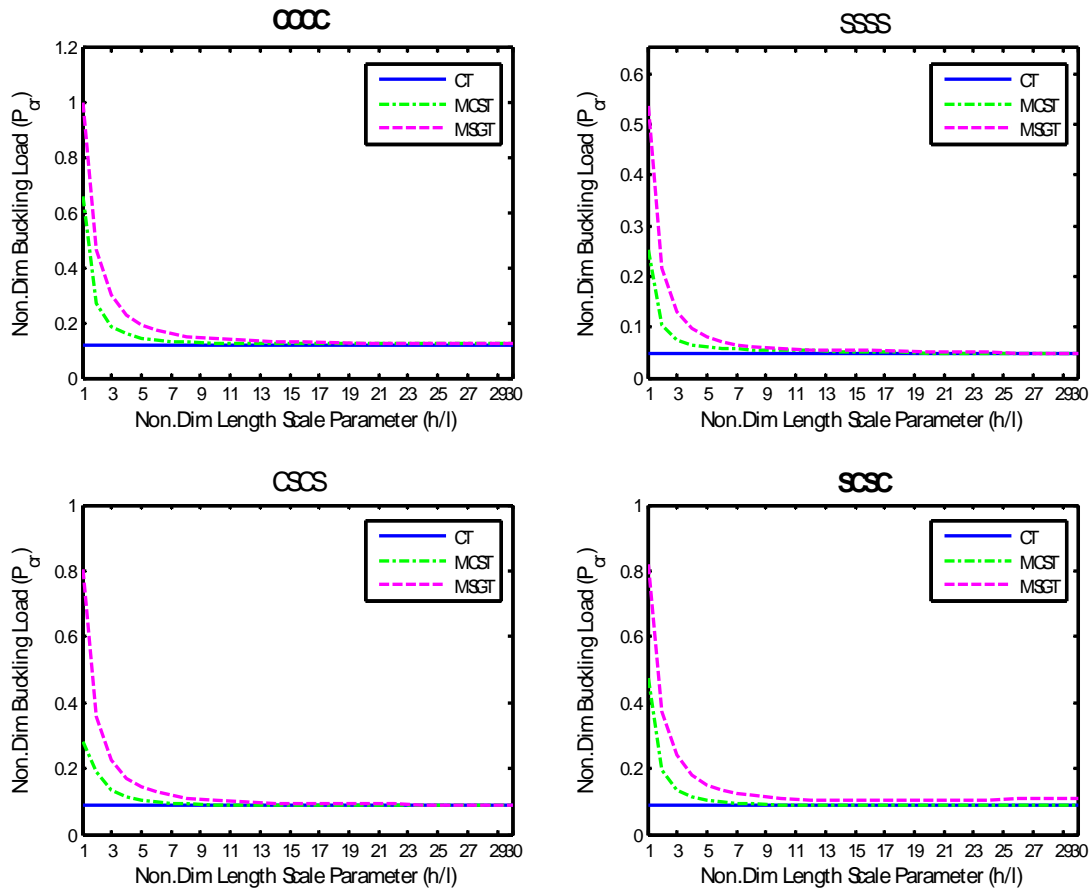


Figure 3: Non-dimensional critical buckling of FG microplate as a function of non-dimensional length scale parameter predicted by CT, MCST and MSGT with $a/h=10$ and $k_{FGM}=0.2$.

Non-dimensional fundamental natural frequency of the FG microplate versus the non-dimensional scale parameter for the three models is plotted in Fig. 4. The trend in variation of the natural frequency is same as that of buckling load so, the similar observations and findings to those of Fig. 3 is found.

Focusing on the results of the last three figures relevant to the different boundary conditions, it is deduced that the most difference between the response predicted by CT and Non-CTs are obtained for the CCCC boundary conditions i.e., the all edges clamped microplate is the most sensitive one to the size effects.

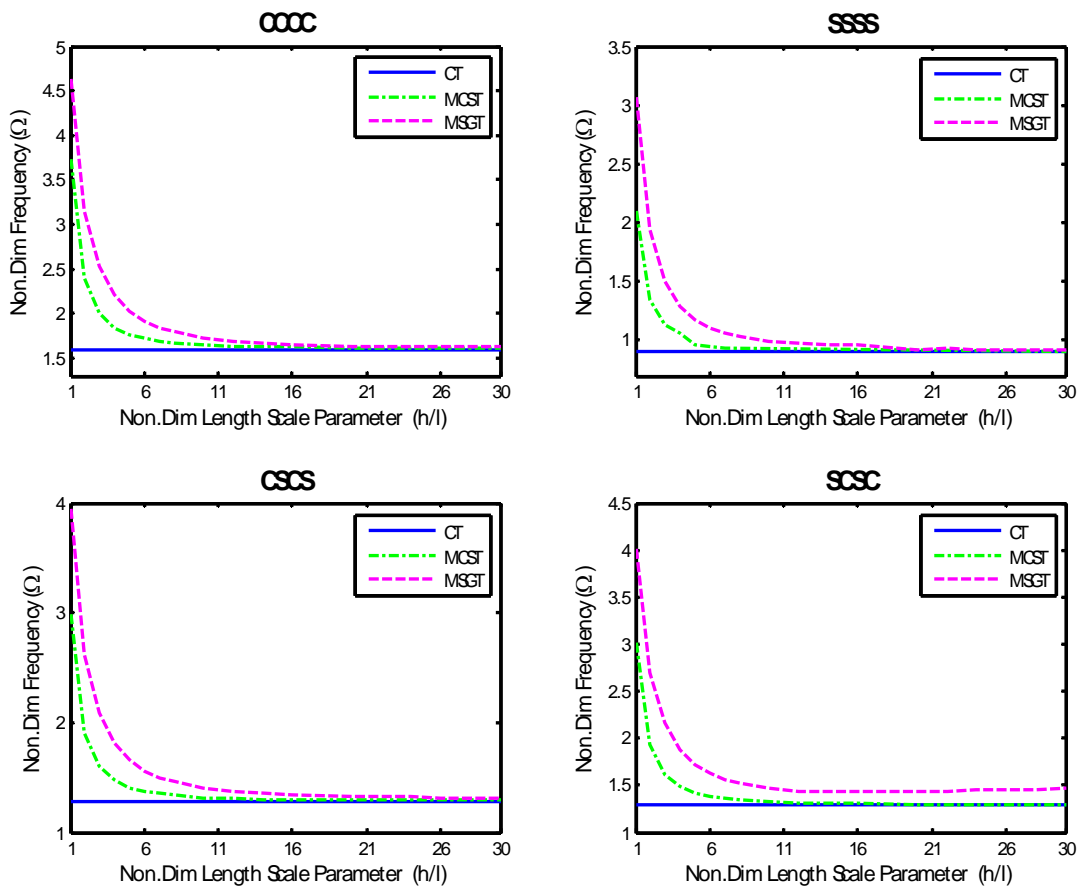


Figure 4: Non-dimensional first natural frequency of FG microplate as a function of non-dimensional length scale parameter predicted by CT, MCST and MSGT with $a/h=10$ and $k_{FGM}=0.2$.

4.2 Material Gradient Index Effects

Indicated in Fig. 5 is the variation of non-dimensional deflection of the FG microplate with material gradient index corresponding to CT, MCST and MSGT. As observed from this figure, as the material gradient exponent increases, the deflection of the microplate increases, too. It is because that an increase in the value of the gradient index causes the volume fraction of the ceramic constituent of FGM to diminishes so, the stiffness of the microplate reduces, too. Further, as expected, for the considered size scale the deflection predicted by the modified stain gradient theory is larger than the two other models. Also, it is found from this figure that the microplate with CCCC and SSSS edge supports have the minimum and maximum deflection, respectively.

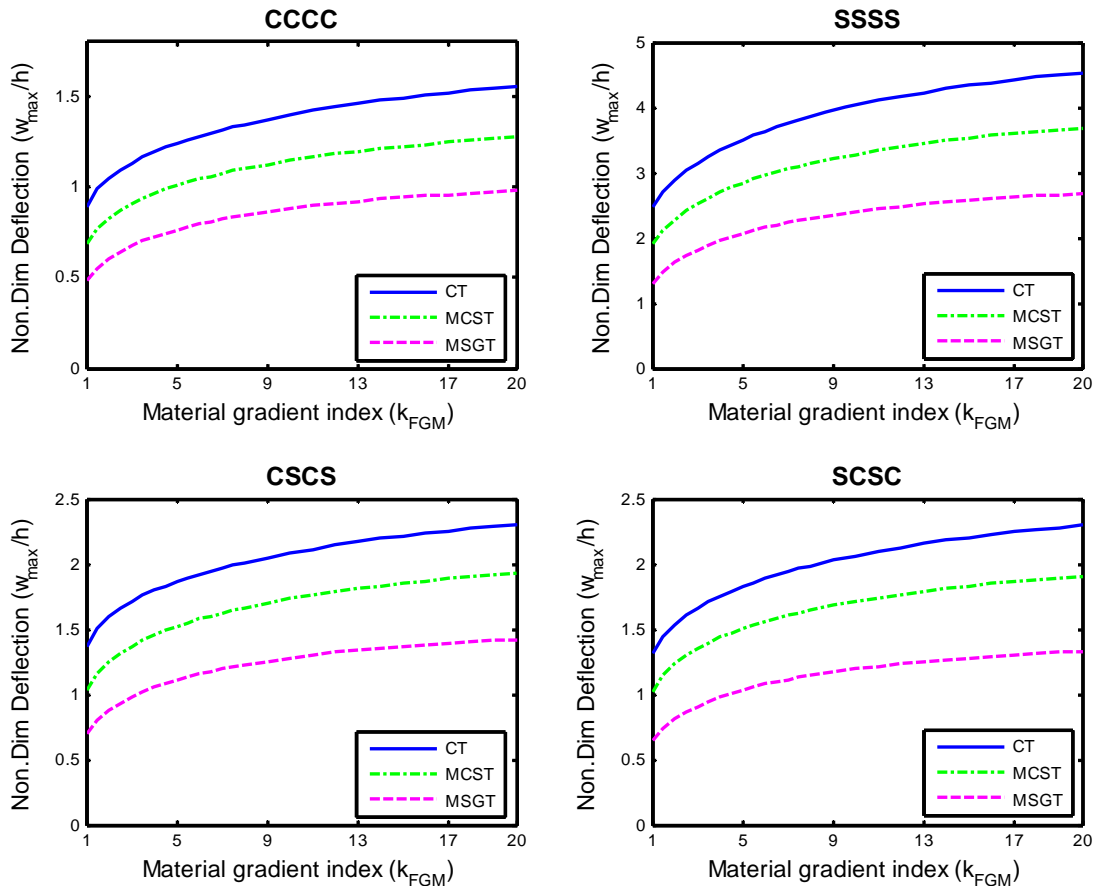


Figure 5: Non-dimensional deflection of FG microplate as a function of material gradient index predicted by CT, MCST and MSGT with $h/l=4$, $a/h = 10$.

Figs. 6 and 7 depict the effect of the material property gradient index predicted by the three models on the non-dimensional critical buckling load and the non-dimensional first natural frequency of the microplate. As shown, both the buckling load and the natural frequency follow a similar pattern based on which they reduce by increasing the value of the gradient index. This trend in variation is against the one corresponding to the non-dimensional deflection of the microplate illustrated in Fig. 5. It is induced by the fact that the reduction of the stiffness of the FG microplate due to the increase of the material gradient index has opposite effect on the deflection and the two eigenvalues namely the critical buckling load and the natural frequency.

From the comparison of the results associated with various boundary conditions, it is discerned that the maximum and minimum buckling load and the natural frequency are obtained for all edges clamped and all edges simply supported microplate, respectively.

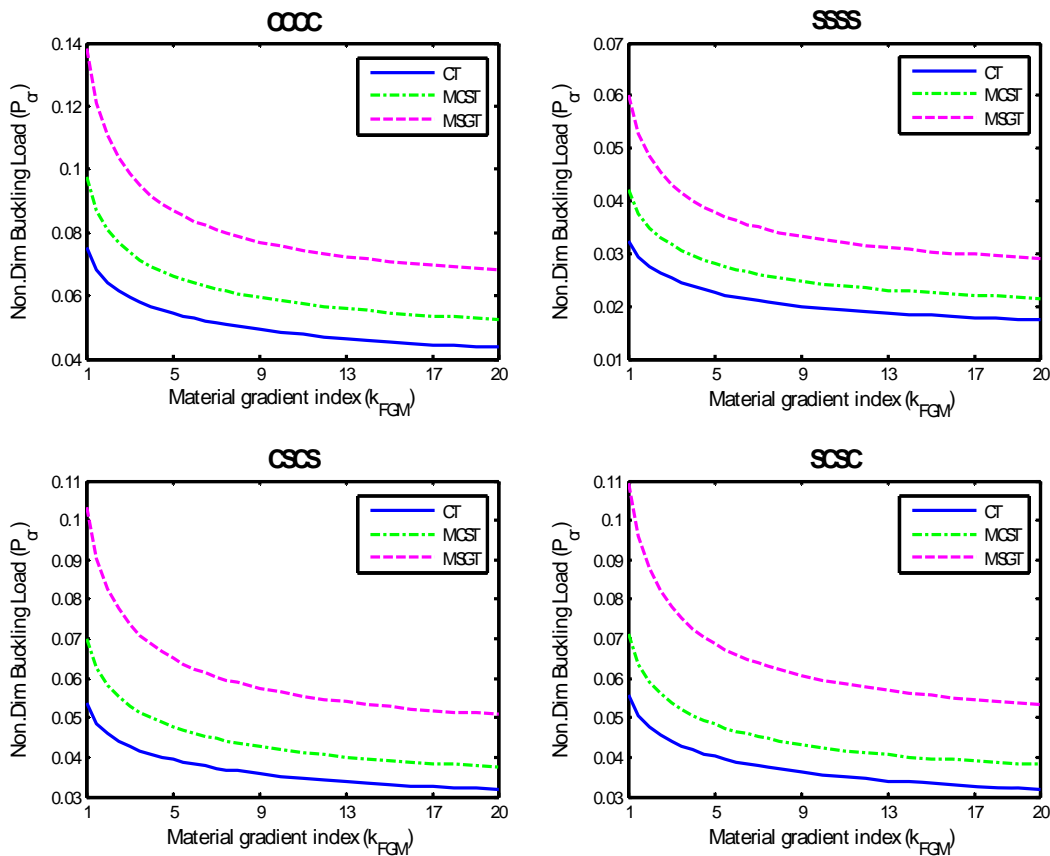
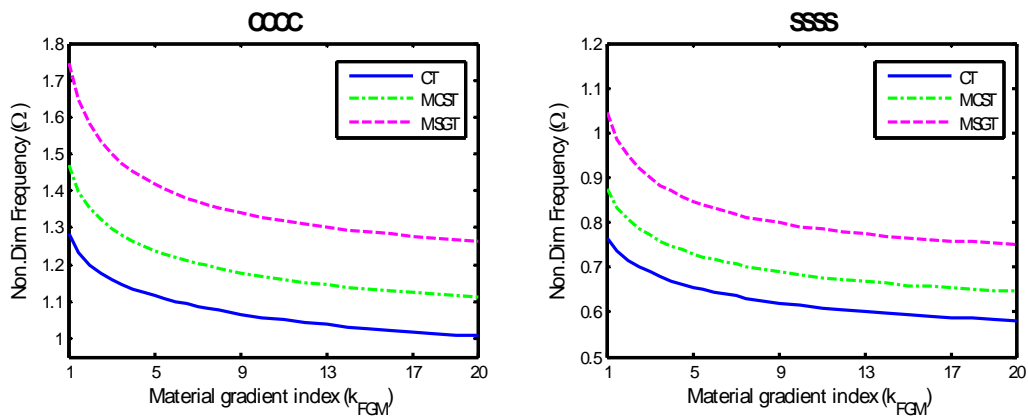


Figure 6: Non-dimensional critical buckling load of FG microplate as a function of material gradient index predicted by CT, MCST and MSGT with $h/l=4$, $a/h = 10$.



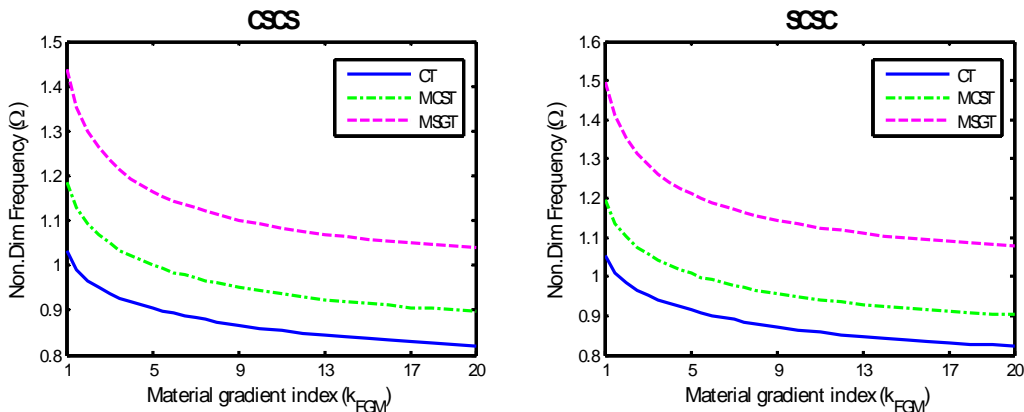
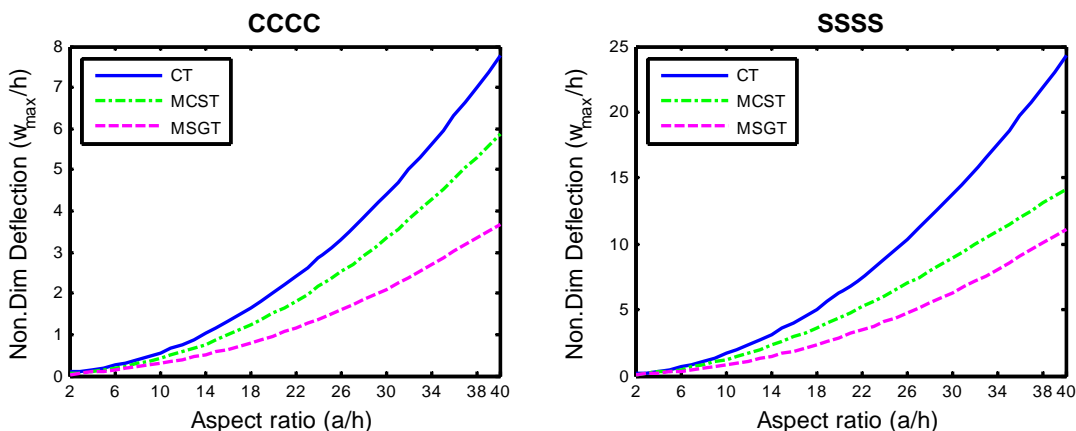


Figure 7: Non-dimensional first natural frequency of FG microplate as a function of material gradient index predicted by CT, MCST and MSGT with $h/l=4$, $a/h = 10$.

4.3 Aspect Ratio Effects

Plotted in Fig. 8 is the Non-dimensional deflection of the FG microplate as a function of aspect ratio (length to thickness of the microplate ratio) for strain gradient theory and the two reduced models. From this figure one can see that going up the aspect ratio leads to an increase in the deflection. Furthermore, for a specific value of a/h , it is observed that the classical theory overpredicts the deflection of the FG microplate. The variation of the non-dimensional critical buckling load and the non-dimensional fundamental natural frequency of the microplate obtained by the classical, the modified couple stress and the modified strain gradient theories with aspect ratio are indicated in Fig. 9 and 10, respectively. A variation trend opposed to that of the deflection shown in the last figure is again observed. Underprediction of the classical theory on the buckling load and the natural frequency is also found.



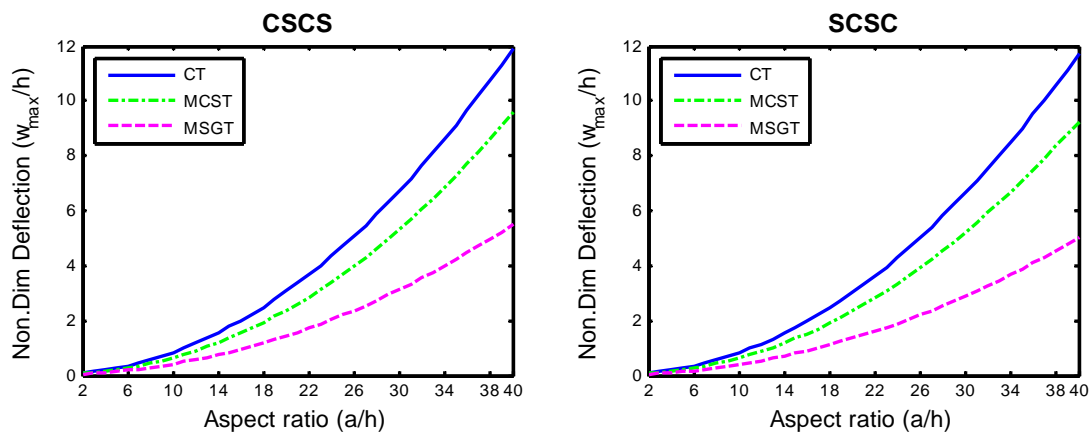


Figure 8: Non-dimensional deflection of FG microplate as a function of aspect ratio predicted by CT, MCST and MSGT with $h/l=4$ and $k_{FGM}=0.2$.

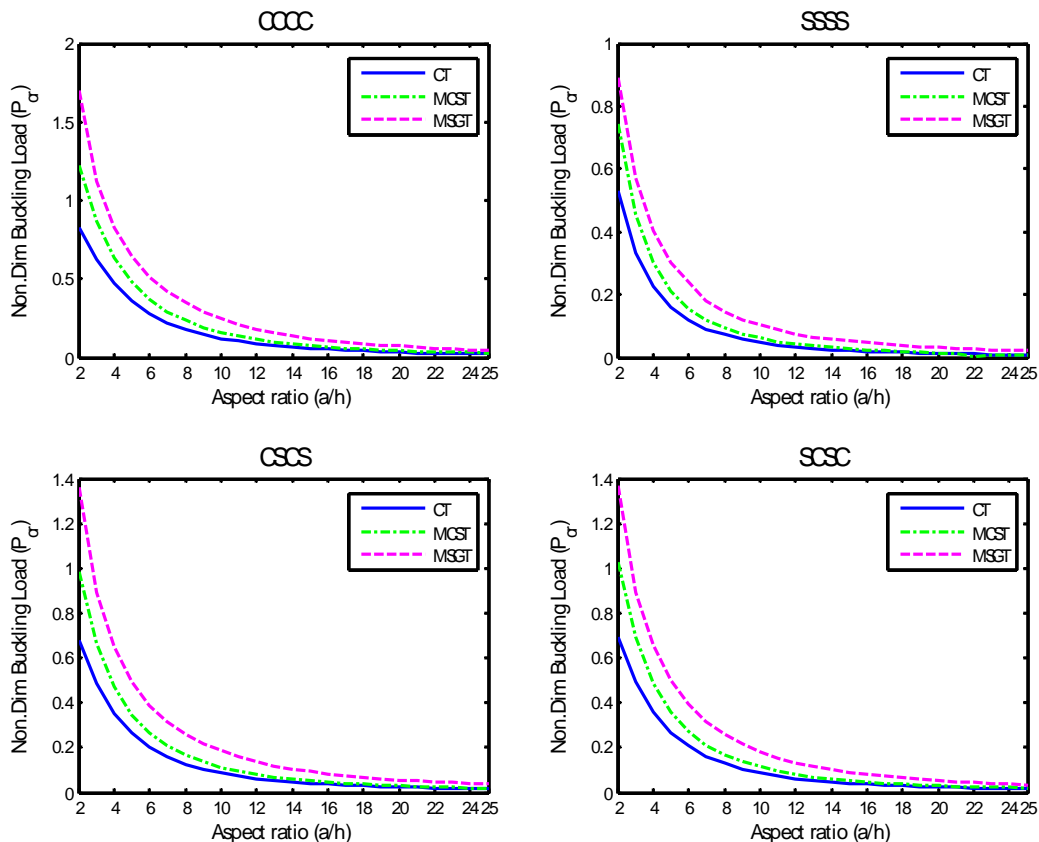


Figure 9: Non-dimensional critical buckling load of FG microplate as a function of aspect ratio predicted by CT, MCST and MSGT with $h/l=4$ and $k_{FGM}=0.2$.

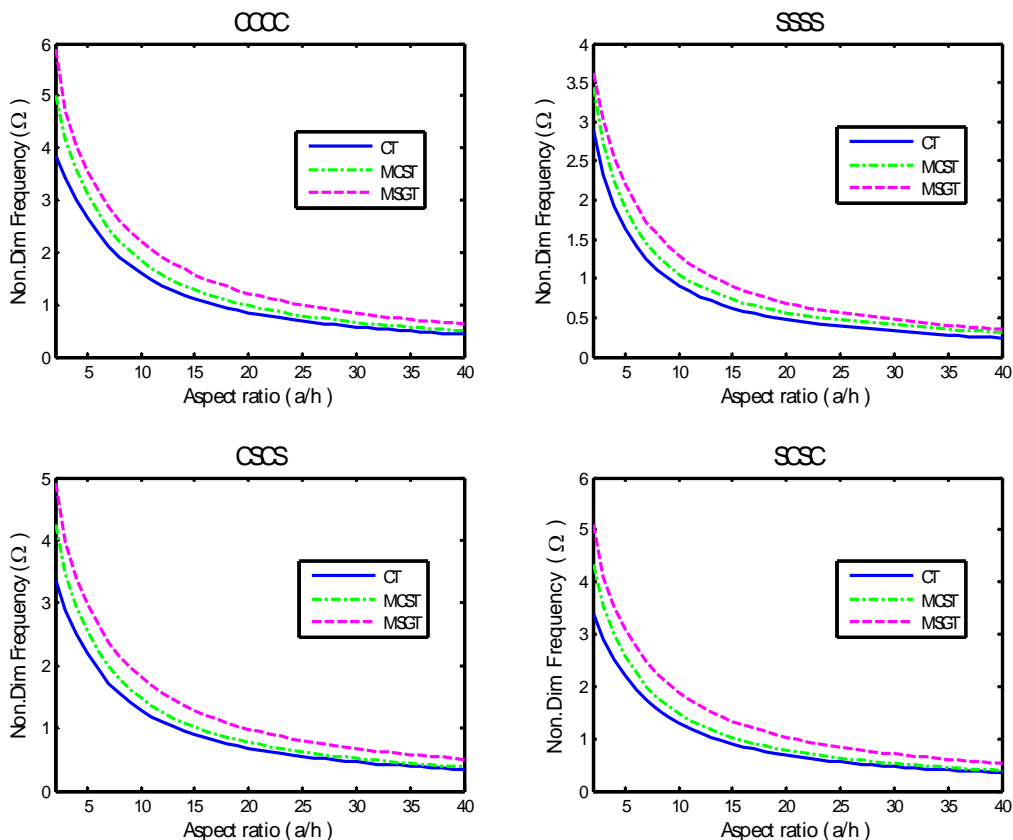


Figure 10: Non-dimensional first natural frequency of FG microplate as a function of aspect ratio predicted by CT, MCST and MSGT with $h/l=4$ and $k_{FGM}=0.2$.

4.4 Thermal Environment Effects

Fig. 11 shows the non-dimensional deflection of FG microplates versus temperature changes predicted by the modified strain gradient theory and the other two reduced theories. It is seen that as the temperature difference increases, the deflection of the microplate goes up too. A contrary behavior is observed for buckling load and natural frequency of the FG microplates in Figs. 12 and 13 where the variation of these quantities with temperature difference is depicted. From these three figures, it is found that the temperature increase due to the thermal environment makes the stiffness of the FG microplate diminish.

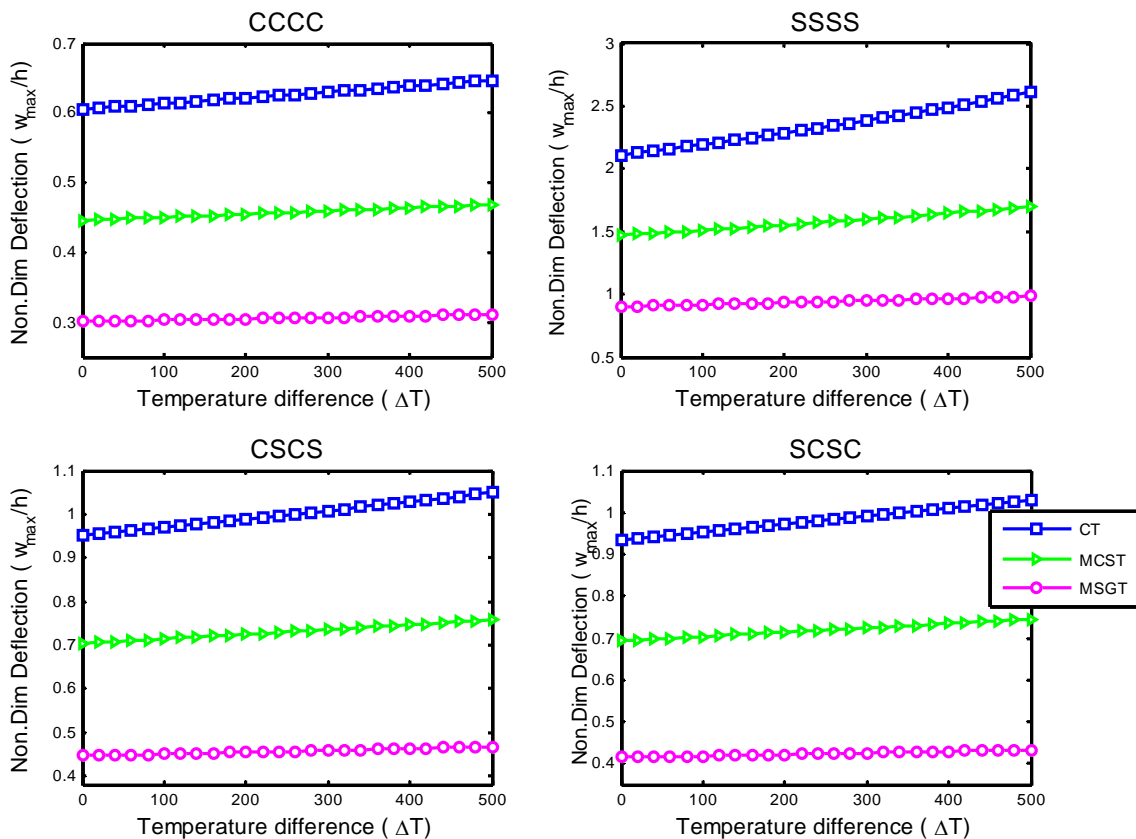
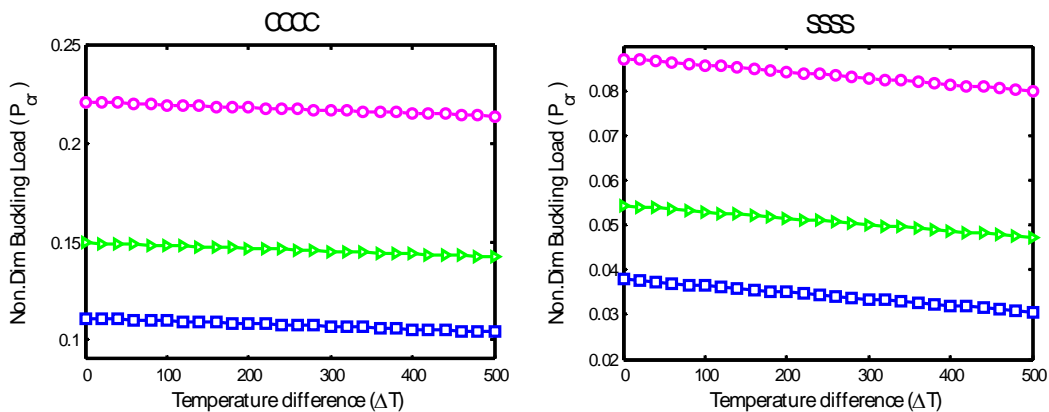


Figure 11: Non-dimensional deflection of FG microplate as a function of temperature difference predicted by CT, MCST and MSGT with $h/l=4$, $a/h = 10$ and $kFGM=0.2$.



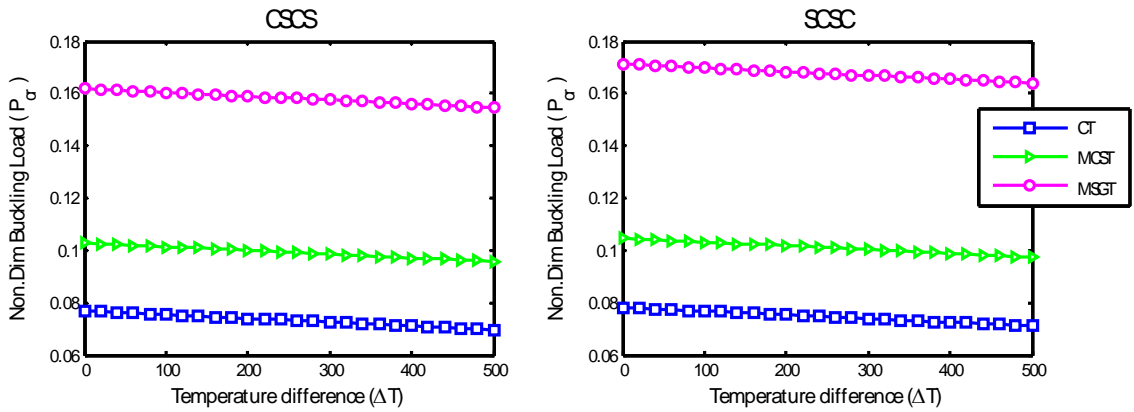


Figure 12: Non-dimensional critical buckling load of FG microplate as a function of temperature difference predicted by CT, MCST and MSGT with $h/l=4$, $a/h = 10$ and $k_{FGM}=0.2$.

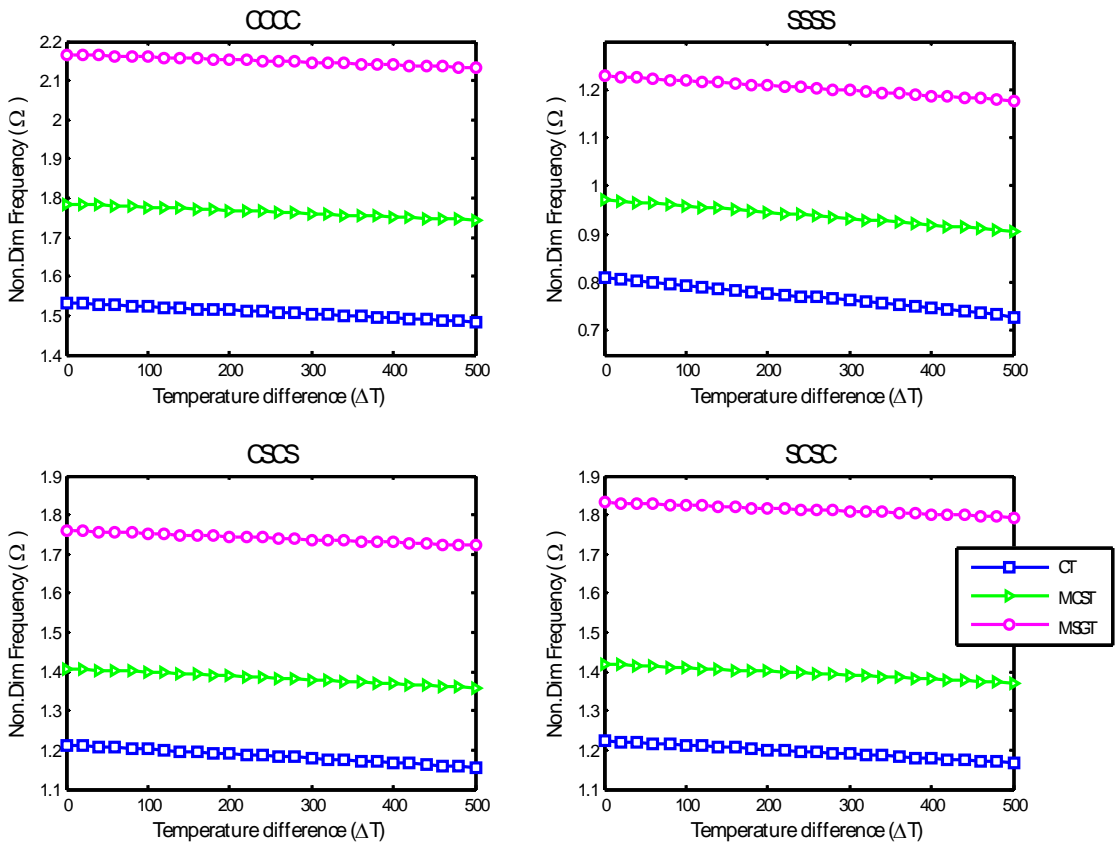


Figure 13: Non-dimensional first natural frequency of FG microplate as a function of temperature difference predicted by CT, MCST and MSGT with $h/l=4$, $a/h = 10$ and $k_{FGM}=0.2$.

5 CONCLUSION

In this paper, the study of bending, buckling and free vibration of the FGM microplate was carried out on the basis of the modified strain gradient and the Mindlin plate theories. The model developed herein accounts for the size effects by incorporating three length scale parameters into the constitutive equations. In addition to MSGT, the numerical results were given for the two other models i.e., CT and MCST constructed by ignoring all or two scale constants in the present model. It was found that the incorporation of the size effect causes increasing the stiffness of the microplate, i.e. decrease of deflection and increase of critical buckling load and natural frequency of the FGM microplate. It was also deduced that size effects become more prominent when MSGT is used and also microplate is subjected to stiffer edge conditions. Moreover, at high structural size, it was observed that the small scale effect becomes less pronounced so that the three models predict approximately the same response. Further, it was discerned that the as the material gradient index and aspect ratio increase, the critical buckling load and fundamental natural frequency decrease and the deflection increases. It was also observed that the thermal environment affects the stiffness of the microplate so that the natural frequency and buckling load of the microscale plate decreases when the temperature increases.

References

- Altan, B. S., & Aifantis, E. C., (1992). On the structure of the mode III crack-tip in gradient elasticity. *Scripta Metallurgica et Materialia* 26: 319–324.
- Ansari, R., Gholami, R., & Darabi, M., (2012). A Nonlinear Timoshenko beam formulation based on strain gradient theory. *Journal of Mechanics of Materials and Structures* 7: 195–211.
- Ansari, R., Gholami, R., Mohammadi, V., & Shojaei, M. F., (2013). Size-dependent Pull-In instability of hydrostatically and electrostatically actuated circular microplates. *Journal of Computational and Nonlinear Dynamics, ASME* 8: 021015.
- Ansari, R., Gholami, R., & Sahmani, S., (2011). Free vibration analysis of size-dependent functionally graded microbeams based on the strain gradient Timoshenko beam theory. *Composite Structures* 94: 221–228.
- Asghari, M., (2012). Geometrically nonlinear micro-plate formulation based on the modified couple stress theory. *International Journal of Engineering Science* 51: 292–309.
- Asghari, M., Rahaeifard, M., Kahrobaiyan, M. H., & Ahmadian, M. T., (2011). The modified couple stress functionally graded Timoshenko beam formulation. *Materials and Design* 32: 1435–1443.
- Chong, A. C. M., & Lam, D. C. C., (1999). Strain gradient plasticity effect in indentation hardness of polymers. *Journal of Materials Research* 14: 4103–4110.
- Fleck, N. A., & Hutchinson, J. W., (1993). A phenomenological theory for strain gradient effects in plasticity. *Journal of the Mechanics and Physics of Solids* 41: 1825–1857.
- Fleck, N. A., Muller, G. M., Ashby, M. F., & Hutchinson, J. W., (1994). Strain gradient plasticity: theory and experiment. *Acta Metallurgica et Materialia* 42: 475–487.
- Jomehzadeh, E., Noori, H. R., & Saidi, A. R., (2011). The size-dependent vibration analysis of micro-plates based on a modified couple stress theory. *Physica E: Low-dimensional Systems and Nanostructures* 43: 877–883.
- Kahrobaiyan, M. H., Asghari, M., Rahaeifard, M., & Ahmadian, M. T., (2010). Investigation of the size-dependent dynamic characteristics of atomic force microscope microcantilevers based on the modified couple stress theory. *International Journal of Engineering Science* 48: 1985–1994.

- Kahrobaian, M. H., Asghari, M., Rahaeifard, M., & Ahmadian, M. T., (2011). A nonlinear strain gradient beam formulation. *International Journal of Engineering Science* 49: 1256–1267.
- Kahrobian, M.H., Rahaeifard, M., Tajalli, S.A., & Ahmadian, M.T., (2012). A strain gradient functionally graded Euler–Bernoulli beam formulation. *International Journal of Engineering Science* 52: 65-76.
- Ke, L. L., Wang, Y. S., & Wang, Z. D., (2011). Thermal effect on free vibration and buckling of size-dependent microbeams. *Physica E: Low-dimensional Systems and Nanostructures* 43: 1387–1393.
- Ke, L. L., Wang, Y. S., Yang, J., & Kitipornchai, S. (2012). Free vibration of size-dependent Mindlin microplates based on the modified couple stress theory. *Journal of Sound and Vibration* 331: 94-106.
- Lam, D. C. C., Yang, F., Chong, A. C. M., Wang, J., & Tong, P., (2003). Experiments and theory in strain gradient elasticity. *Journal of the Mechanics and Physics of Solids* 51: 1477–1508.
- Lazopoulos, K. A., (2004). On the gradient strain elasticity theory of plates. *European Journal of Mechanics*, 23, 843–852.
- Lazopoulos, K. A., (2009). On bending of strain gradient elastic micro-plates. *Mechanics Research Communications* 36: 777–783.
- Ma, H. M., Gao, X.-L., & Reddy, J. N., (2008). A microstructure-dependent Timoshenko beam model based on a modified couple stress theory. *Journal of the Mechanics and Physics of Solids* 56: 3379–3391.
- Ma, Q., & Clarke, D. R., (1995). Size dependent hardness of silver single crystals. *Journal of Materials Research*, 10, 853–863.
- McFarland, A. W., & Colton, J. S., (2005). Role of material microstructure in plate stiffness with relevance to microcantilever sensors. *Journal of Micromechanics and Microengineering* 15: 1060–1067.
- Mindlin, R. D., (1965). Second gradient of strain and surface tension in linear elasticity. *International Journal of Solids and Structures* 1: 417–438.
- Mindlin, R. D., & Tiersten, H. F., (1962). Effects of couple-stresses in linear elasticity. *Archs Rational Mechanics Analysis* 11: 415–448.
- Nateghi, A., Salamat-talab, M., Rezapour, J., & Daneshian, B., (2012). Size dependent buckling analysis of functionally graded micro beams based on modified couple stress theory. *Applied Mathematical Modelling* 36: 4971–4987.
- Nix, W. D., (1989). Mechanical-properties of thin-films. *Metallurgical Transactions A-Physical Metallurgy and Materials Science* 20: 2217–2245.
- Papargyri-Beskou, S., & Beskos, D. E., (2008). Static, stability and dynamic analysis of gradient elastic flexural Kirchhoff plates. *Archive of Applied Mechanics* 78: 625–635.
- Papargyri-Beskou, S., Giannakopoulos, A. E., & Beskos, D. E., (2010). Variational analysis of gradient elastic flexural plates under static loading. *International Journal of Solids and Structures* 47: 2755–2766.
- Papargyri-Beskou, S., Tsepoura, K. G., Polyzos, D., & Beskos, D. E., (2003). Bending and stability analysis of gradient elastic beams. *International Journal of Solids and Structures* 40: 385–400.
- Sahmani, S., & Ansari, R., (2013). On the free vibration response of functionally graded higher-order shear deformable microplates based on the strain gradient elasticity theory. *Composite Structures* 95: 430–442.
- Stolken, J. S., & Evans, A. G., (1998). Microbend test method for measuring the plasticity length scale. *Acta Materialia* 46: 5109–5115.
- Thai, H. T., & Choi, D. H., (2013). Size-dependent functionally graded Kirchhoff and Mindlin plate models based on a modified couple stress theory. *Composite Structures* 95: 142–153.
- Toupin, R. A., (1964). Theories of elasticity with couple-stress. *Archs Rational Mechanics Analysis*, 17, 85–112.
- Tsiatas, G. C., (2009). A new Kirchhoff plate model based on a modified couple stress theory. *International Journal of Solids and Structures* 46: 2757–2764.

Vardoulakis, I., Exadaktylos, G., & Kourkoulis, S. K., (1998). Bending of marble with intrinsic length scales: a gradient theory with surface energy and size effects. *Journal de Physique IV* 8: 399–406.

Wang, B., Zhou, S., Zhao, J., & Chen, X., (2011). A size-dependent Kirchhoff micro-plate model based on strain gradient elasticity Theory. *European Journal of Mechanics - A/Solids* 30: 517–524.

Yang, F., Chong, A. C. M., Lam, D. C. C., & Tong, P., (2002). Couple stress based strain gradient theory for elasticity. *International Journal of Solids and Structures* 39: 2731–2743.

Yin, L. Qian, Q. Wang, L., & Xia, W., (2010). Vibration analysis of microscale plates based on modified couple stress theory. *Acta Mechanica Solida Sinica* 23: 386-393.

Appendix A

$$\begin{aligned} \tilde{N}_{xx} &= N_{xx} + \frac{1}{4} \frac{\partial Y_{xz}}{\partial y} - \frac{\partial P_x}{\partial x} - \frac{1}{2} \frac{\partial P_y}{\partial y} - \frac{\partial T_{xxx}}{\partial x} - \frac{\partial T_{xyy}}{\partial y}, \\ \tilde{N}_{xy} &= N_{xy} + \frac{1}{4} \frac{\partial Y_{xz}}{\partial x} + \frac{1}{2} \frac{\partial Y_{yz}}{\partial y} - \frac{1}{2} \frac{\partial P_y}{\partial x} - \frac{\partial T_{yyx}}{\partial y} - \frac{\partial T_{xxy}}{\partial x}, \\ \tilde{N}_{yx} &= N_{yx} - \frac{1}{4} \frac{\partial Y_{yz}}{\partial y} - \frac{1}{2} \frac{\partial Y_{xz}}{\partial x} - \frac{1}{2} \frac{\partial P_x}{\partial y} - \frac{\partial T_{xxy}}{\partial x} - \frac{\partial T_{yyx}}{\partial y}, \\ \tilde{N}_{yy} &= N_{yy} - \frac{1}{4} \frac{\partial Y_{yz}}{\partial x} - \frac{\partial P_y}{\partial y} - \frac{1}{2} \frac{\partial P_x}{\partial x} - \frac{\partial T_{yyy}}{\partial y} - \frac{\partial T_{yyx}}{\partial x}, \\ \tilde{Q}_x &= Q_x - \frac{\partial T_{zzz}}{\partial x} - \frac{1}{4} \left(\frac{\partial Y_{xx}}{\partial y} - \frac{\partial Y_{yy}}{\partial y} - 2 \frac{\partial Y_{xy}}{\partial x} \right) - \frac{\partial T_{xyz}}{\partial y}, \\ \tilde{Q}_y &= Q_y - \frac{\partial T_{yyz}}{\partial y} - \frac{1}{4} \left(\frac{\partial Y_{xx}}{\partial x} - \frac{\partial Y_{yy}}{\partial x} + 2 \frac{\partial Y_{xy}}{\partial y} \right) - \frac{\partial T_{xyz}}{\partial x}, \\ \tilde{M}_{xx} &= M_{xx} + \frac{1}{4} \left(2Y_{xy} + \frac{\partial H_{xz}}{\partial y} \right) + P_z - \frac{1}{2} \left(2 \frac{\partial M_x^p}{\partial x} + \frac{\partial M_y^p}{\partial y} \right) + 2T_{zzz}^r - \frac{\partial M_{xxx}}{\partial x} - \frac{\partial M_{xxy}}{\partial y}, \\ \tilde{M}_{xy} &= M_{xy} + \frac{Y_{yy} - Y_{zz}}{2} + \frac{1}{4} \left(2 \frac{\partial H_{yz}}{\partial y} + \frac{\partial H_{xz}}{\partial x} \right) + 2T_{xyz} - \frac{1}{2} \frac{\partial M_y^p}{\partial x} - \frac{\partial M_{yyx}}{\partial y} - \frac{\partial M_{xxy}}{\partial x}, \\ \tilde{M}_{yx} &= M_{yx} + \frac{Y_{zz} - Y_{xx}}{2} - \frac{1}{4} \left(2 \frac{\partial H_{xz}}{\partial x} + \frac{\partial H_{yz}}{\partial y} \right) - \frac{\partial M_{xxy}}{\partial x} + 2T_{xyz} - \frac{1}{2} \frac{\partial M_x^p}{\partial y} - \frac{\partial M_{yyx}}{\partial y}, \\ \tilde{M}_{yy} &= M_{yy} - \frac{\partial M_y^p}{\partial y} + P_z - \frac{1}{2} Y_{xy} + 2T_{yyz} - \frac{\partial M_{yyy}}{\partial y} - \frac{1}{4} \frac{\partial H_{yz}}{\partial x} - \frac{1}{2} \frac{\partial M_x^p}{\partial x} - \frac{\partial M_{yyx}}{\partial x}. \end{aligned}$$

1. Transverse force vector in the bending problem

$$\mathbf{q} = [0 \ 0 \ 1 \ 0 \ 0]^T$$

Note that \mathbf{q} is a $5NM \times 1$ vector.

2. Stiffness matrix in the bending, buckling and free vibration problems

$$\mathbf{K} = \begin{bmatrix} \mathbf{k}_{11} & \mathbf{k}_{12} & \mathbf{k}_{13} & \mathbf{k}_{14} & \mathbf{k}_{15} \\ \mathbf{k}_{21} & \mathbf{k}_{22} & \mathbf{k}_{23} & \mathbf{k}_{24} & \mathbf{k}_{25} \\ \mathbf{k}_{31} & \mathbf{k}_{32} & \mathbf{k}_{33} & \mathbf{k}_{34} & \mathbf{k}_{35} \\ \mathbf{k}_{41} & \mathbf{k}_{42} & \mathbf{k}_{43} & \mathbf{k}_{44} & \mathbf{k}_{45} \\ \mathbf{k}_{51} & \mathbf{k}_{52} & \mathbf{k}_{53} & \mathbf{k}_{54} & \mathbf{k}_{55} \end{bmatrix}$$

in which

$$\begin{aligned} \mathbf{k}_{11} &= a_{11}\mathbf{I}_\zeta \otimes \mathbf{D}_\xi^{(2)} + a_{55}\kappa^2\mathbf{D}_\zeta^{(2)} \otimes \mathbf{I}_\xi - \frac{c_1}{\eta_1^2}a_{55}\mathbf{I}_\zeta \otimes \mathbf{D}_\xi^{(4)} - \frac{c_2\kappa^4}{\eta_1^2}a_{55}\mathbf{D}_\zeta^{(4)} \otimes \mathbf{I}_\xi - \frac{c_3\kappa^2}{\eta_1^2}a_{55}\mathbf{D}_\zeta^{(2)} \otimes \mathbf{D}_\xi^{(2)}, \\ \mathbf{k}_{12} = \mathbf{k}_{21} &= (a_{12} + a_{55})\kappa\mathbf{D}_\zeta^{(1)} \otimes \mathbf{D}_\xi^{(1)} - \frac{a_{55}c_4\kappa}{\eta_1^2}(\mathbf{D}_\zeta^{(1)} \otimes \mathbf{D}_\xi^{(3)} + \kappa^2\mathbf{D}_\zeta^{(3)} \otimes \mathbf{D}_\xi^{(1)}), & \mathbf{k}_{13} = \mathbf{k}_{23} &= 0, \\ \mathbf{k}_{14} = \mathbf{k}_{41} &= b_{11}\mathbf{I}_\zeta \otimes \mathbf{D}_\xi^{(2)} + b_{55}\kappa^2\mathbf{D}_\zeta^{(2)} \otimes \mathbf{I}_\xi - \frac{c_1}{\eta_1^2}b_{55}\mathbf{I}_\zeta \otimes \mathbf{D}_\xi^{(4)} - \frac{c_2\kappa^4}{\eta_1^2}b_{55}\mathbf{D}_\zeta^{(4)} \otimes \mathbf{I}_\xi - \frac{c_3\kappa^2}{\eta_1^2}b_{55}\mathbf{D}_\zeta^{(2)} \otimes \mathbf{D}_\xi^{(2)}, \\ \mathbf{k}_{15} = \mathbf{k}_{51} &= (b_{12} + b_{55})\kappa\mathbf{D}_\zeta^{(1)} \otimes \mathbf{D}_\xi^{(1)} - \frac{b_{55}c_4\kappa}{\eta_1^2}(\mathbf{D}_\zeta^{(1)} \otimes \mathbf{D}_\xi^{(3)} + \kappa^2\mathbf{D}_\zeta^{(3)} \otimes \mathbf{D}_\xi^{(1)}), \\ \mathbf{k}_{22} &= a_{11}\kappa^2\mathbf{D}_\zeta^{(2)} \otimes \mathbf{I}_\xi + a_{55}\mathbf{I}_\zeta \otimes \mathbf{D}_\xi^{(2)} - \frac{c_1\kappa^4}{\eta_1^2}a_{55}\mathbf{D}_\zeta^{(4)} \otimes \mathbf{I}_\xi - \frac{c_2}{\eta_1^2}a_{55}\mathbf{I}_\zeta \otimes \mathbf{D}_\xi^{(4)} - \frac{c_3\kappa^2}{\eta_1^2}a_{55}\mathbf{D}_\zeta^{(2)} \otimes \mathbf{D}_\xi^{(2)}, \\ \mathbf{k}_{24} = \mathbf{k}_{42} &= (b_{12} + b_{55})\kappa\mathbf{D}_\zeta^{(1)} \otimes \mathbf{D}_\xi^{(1)} - \frac{b_{55}c_4\kappa}{\eta_1^2}(\mathbf{D}_\zeta^{(1)} \otimes \mathbf{D}_\xi^{(3)} + \kappa^2\mathbf{D}_\zeta^{(3)} \otimes \mathbf{D}_\xi^{(1)}), & \mathbf{k}_{31} = \mathbf{k}_{32} &= 0, \\ \mathbf{k}_{33} &= k_s a_{55}(\mathbf{I}_\zeta \otimes \mathbf{D}_\xi^{(2)} + \kappa^2\mathbf{D}_\zeta^{(2)} \otimes \mathbf{I}_\xi) - \frac{a_{55}c_2}{\eta_1^2}(\mathbf{I}_\zeta \otimes \mathbf{D}_\xi^{(4)} + 2\kappa^2\mathbf{D}_\zeta^{(2)} \otimes \mathbf{D}_\xi^{(2)} + \kappa^4\mathbf{D}_\zeta^{(4)} \otimes \mathbf{I}_\xi) - N_T(\mathbf{I}_\zeta \otimes \mathbf{D}_\xi^{(2)} + \kappa^2\mathbf{D}_\zeta^{(2)} \otimes \mathbf{I}_\xi), \\ \mathbf{k}_{34} = -\mathbf{k}_{43} &= k_s a_{55}\eta_1\mathbf{I}_\zeta \otimes \mathbf{D}_\xi^{(1)} - \frac{a_{55}c_5}{\eta_1}(\mathbf{I}_\zeta \otimes \mathbf{D}_\xi^{(3)} + \kappa^2\mathbf{D}_\zeta^{(2)} \otimes \mathbf{D}_\xi^{(1)}), \\ \mathbf{k}_{35} = -\mathbf{k}_{53} &= k_s a_{55}\kappa\eta_1\mathbf{D}_\zeta^{(1)} \otimes \mathbf{I}_\xi - \frac{a_{55}c_5}{\eta_1}(\kappa\mathbf{D}_\zeta^{(1)} \otimes \mathbf{D}_\xi^{(2)} + \kappa^3\mathbf{D}_\zeta^{(3)} \otimes \mathbf{I}_\xi), \\ \mathbf{k}_{44} &= d_{11}\mathbf{I}_\zeta \otimes \mathbf{D}_\xi^{(2)} + d_{55}\kappa^2\mathbf{D}_\zeta^{(2)} \otimes \mathbf{I}_\xi - k_s a_{55}\eta_1^2\mathbf{I}_\zeta \otimes \mathbf{I}_\xi - \frac{c_1}{\eta_1^2}d_{55}\mathbf{I}_\zeta \otimes \mathbf{D}_\xi^{(4)} - \frac{c_2\kappa^4}{\eta_1^2}d_{55}\mathbf{D}_\zeta^{(4)} \otimes \mathbf{I}_\xi \\ &\quad - \frac{c_3\kappa^2}{\eta_1^2}d_{55}\mathbf{D}_\zeta^{(2)} \otimes \mathbf{D}_\xi^{(2)} + a_{55}c_6(\mathbf{I}_\zeta \otimes \mathbf{D}_\xi^{(2)} + \kappa^2\mathbf{D}_\zeta^{(2)} \otimes \mathbf{I}_\xi) - a_{55}c_7\kappa^2\mathbf{D}_\zeta^{(2)} \otimes \mathbf{I}_\xi, \\ \mathbf{k}_{45} = \mathbf{k}_{54} &= (d_{12} + d_{55})\kappa\mathbf{D}_\zeta^{(1)} \otimes \mathbf{D}_\xi^{(1)} - \frac{d_{55}c_4\kappa}{\eta_1^2}(\mathbf{D}_\zeta^{(1)} \otimes \mathbf{D}_\xi^{(3)} + \kappa^2\mathbf{D}_\zeta^{(3)} \otimes \mathbf{D}_\xi^{(1)}) + a_{55}c_7\kappa\mathbf{D}_\zeta^{(1)} \otimes \mathbf{D}_\xi^{(1)}, \end{aligned}$$

$$\mathbf{k}_{55} = d_{11}\kappa^2\mathbf{D}_{\zeta}^{(2)} \otimes \mathbf{I}_{\xi} + d_{55}\mathbf{I}_{\zeta} \otimes \mathbf{D}_{\xi}^{(2)} - k_s a_{55}\eta_1^2\mathbf{I}_{\zeta} \otimes \mathbf{I}_{\xi} - \frac{c_1\kappa^4}{\eta_1^2}d_{55}\mathbf{D}_{\zeta}^{(4)} \otimes \mathbf{I}_{\xi} - \frac{c_2}{\eta_1^2}d_{55}\mathbf{I}_{\zeta} \otimes \mathbf{D}_{\xi}^{(4)}$$

$$- \frac{c_3\kappa^2}{\eta_1^2}d_{55}\mathbf{D}_{\zeta}^{(2)} \otimes \mathbf{D}_{\xi}^{(2)} + a_{55}c_6 \left(\mathbf{I}_{\zeta} \otimes \mathbf{D}_{\xi}^{(2)} + \kappa^2\mathbf{D}_{\zeta}^{(2)} \otimes \mathbf{I}_{\xi} \right) - a_{55}c_7\mathbf{I}_{\zeta} \otimes \mathbf{D}_{\xi}^{(2)},$$

$$\mathbf{k}_{25} = \mathbf{k}_{52} = b_{11}\kappa^2\mathbf{D}_{\zeta}^{(2)} \otimes \mathbf{I}_{\xi} + b_{55}\mathbf{I}_{\zeta} \otimes \mathbf{D}_{\xi}^{(2)} - \frac{c_1\kappa^4}{\eta_1^2}b_{55}\mathbf{D}_{\zeta}^{(4)} \otimes \mathbf{I}_{\xi} - \frac{c_2}{\eta_1^2}b_{55}\mathbf{I}_{\zeta} \otimes \mathbf{D}_{\xi}^{(4)} - \frac{c_3\kappa^2}{\eta_1^2}b_{55}\mathbf{D}_{\zeta}^{(2)} \otimes \mathbf{D}_{\xi}^{(2)},$$

3. Matrix **N** in the buckling problem

$$\mathbf{N} = \begin{bmatrix} \mathbf{0} & \mathbf{0} & \mathbf{0} & & \mathbf{0} & \mathbf{0} \\ \mathbf{0} & \mathbf{0} & \mathbf{0} & & \mathbf{0} & \mathbf{0} \\ \mathbf{0} & \mathbf{0} & \mathbf{I}_{\zeta} \otimes \mathbf{D}_{\xi}^{(2)} + \kappa^2\mathbf{D}_{\zeta}^{(2)} \otimes \mathbf{I}_{\xi} & & \mathbf{0} & \mathbf{0} \\ \mathbf{0} & \mathbf{0} & \mathbf{0} & & \mathbf{0} & \mathbf{0} \\ \mathbf{0} & \mathbf{0} & \mathbf{0} & & \mathbf{0} & \mathbf{0} \end{bmatrix}$$

4. Mass matrix in the free vibration problem

$$\mathbf{M} = \begin{bmatrix} \bar{I}_0\mathbf{I}_{\zeta} \otimes \mathbf{I}_{\xi} & \mathbf{0} & \mathbf{0} & \bar{I}_1\mathbf{I}_{\zeta} \otimes \mathbf{I}_{\xi} & \mathbf{0} \\ \mathbf{0} & \bar{I}_0\mathbf{I}_{\zeta} \otimes \mathbf{I}_{\xi} & \mathbf{0} & \mathbf{0} & \bar{I}_1\mathbf{I}_{\zeta} \otimes \mathbf{I}_{\xi} \\ \mathbf{0} & \mathbf{0} & \bar{I}_0\mathbf{I}_{\zeta} \otimes \mathbf{I}_{\xi} & \mathbf{0} & \mathbf{0} \\ \bar{I}_1\mathbf{I}_{\zeta} \otimes \mathbf{I}_{\xi} & \mathbf{0} & \mathbf{0} & \bar{I}_2\mathbf{I}_{\zeta} \otimes \mathbf{I}_{\xi} & \mathbf{0} \\ \mathbf{0} & \bar{I}_1\mathbf{I}_{\zeta} \otimes \mathbf{I}_{\xi} & \mathbf{0} & \mathbf{0} & \bar{I}_2\mathbf{I}_{\zeta} \otimes \mathbf{I}_{\xi} \end{bmatrix}$$